Redefining Ormyridae (Hymenoptera, Chalcidoidea) with establishment of subfamilies and description of new genera

Simon van Noort, Mircea-dan Mitroiu, Roger Burks, Gary Gibson, Paul Hanson, John Heraty, Petr Janšta, Astrid Cruaud, Jean-yves Rasplus

ORIGINAL ARTICLE

Redefining Ormyridae (Hymenoptera, Chalcidoidea) with establishment of subfamilies and description of new genera

Simon van Noort[1,2] | Mircea-Dan Mitroiu[3] | Roger Burks[4] |
Gary Gibson[5] | Paul Hanson[6] | John Heraty[7] | Petr Janšta[8,9] |
Astrid Cruaud[10] | Jean-Yves Rasplus[10]

[1]Research and Exhibitions Department, South African Museum, Iziko Museums of South Africa, Cape Town, South Africa

[2]Department of Biological Sciences, University of Cape Town, Cape Town, South Africa

[3]Faculty of Biology, Alexandru Ioan Cuza University of Iași, Iași, Romania

[4]Riverside Department of Entomology, University of California, Riverside, California, USA

[5]Honorary Research Associate, Agriculture and Agri-Food Canada, Canadian National Collection of Insects, Arachnids and Nematodes, Ottawa, Ontario, Canada

[6]School of Biology, University of Costa Rica, San Jose, Costa Rica

[7]Department of Entomology, University of California, Riverside, California, USA

[8]Department of Zoology, Faculty of Science, Charles University, Prague, Czech Republic

[9]Department of Entomology, State Museum of Natural History, Stuttgart, Germany

[10]CBGP, Center for Biology and Management of Populations, INRAE, CIRAD, IRD, Montpellier SupAgro, University Montpellier, Montpellier, France

Correspondence
Simon van Noort, Research and Exhibitions Department, South African Museum, Iziko Museums of South Africa, Cape Town, South Africa.
Email: svannoort@iziko.org.za

Funding information
Institut National de Recherche pour l'Agriculture, l'Alimentation et l'Environnement; National Research Foundation, Grant/Award Numbers: GUN 61497, GUN 79004, GUN 79211, GUN 81139, GUN 98115, GUN 2068865

Abstract

The circumscription of the family Ormyridae (Hymenoptera: Chalcidoidea) is revised after phylogenetic analysis based on ultra-conserved elements (UCEs) and comparative morphological assessment of the chalcid 'Gall Clade'. Six genera are treated in the family, including two new genera, *Halleriaphagus* van Noort and Burks, **gen. nov.**, and *Ouma* Mitroiu, **gen. nov.** One genus, *Eubeckerella* Narendran, is re-assigned to the family, and *Ormyrulus* Bouček is synonymised with *Ormyrus* Westwood, **syn. nov.**, resulting in the new combination *Ormyrus gibbus* (Bouček), **comb. nov.** The six genera are classified in three subfamilies, two of which are newly described, Asparagobiinae van Noort, Burks, Mitroiu and Rasplus, **subfam. nov.,** and Hemadinae van Noort, Burks, Mitroiu and Rasplus, **subfam. nov.** *Halleriaphagus* is established for the newly described type species *Halleriaphagus phagolucida* van Noort and Burks, **sp. nov.**, and *Ouma* is erected for *O. daleskeyae* Mitroiu, **sp. nov.**, and *O. emazantsi* Mitroiu, **sp. nov.** *Asparagobius* is revised with description of *Asparagobius bouceki* van Noort, **sp. nov.**, and *Asparagobius copelandi* Rasplus and van Noort, **sp. nov.** *Asparagobius* and *Halleriaphagus* are classified in Asparagobiinae, *Hemadas* in Hemadinae and *Eubeckerella*, *Ormyrus* and *Ouma* in Ormyrinae. The molecular support defining

Astrid Cruaud and Jean-Yves Rasplus contributed equally.

- -

the ormyrid clade is corroborated by the proposed morphological synapomorphy of a foliaceous prepectus overlying the tegula base. Identification keys to the genera of Ormyridae and to the species of *Asparagobius* and *Ouma* are provided. Online Lucid identification keys and images of all the species treated herein are available at: http://www.waspweb.org.

Zoobank Registration: LSID urn:lsid:zoobank.org:pub:8811695B-EE57-4C18-A6B6-E63D267E2373.

INTRODUCTION

According to the recently revised classification of Chalcidoidea by Burks et al. (2022) and Cruaud et al. (2024), most chalcidoid gall-associates are placed in the families Cynipencyrtidae, Epichrysomallidae, Melanosomellidae, Ormyridae and Tanaostigmatidae (Burks et al., 2022). Together, these taxa comprise the so called 'Gall Clade' sensu Burks et al. (2022) and Cruaud et al. (2024). Cynipencyrtidae contains two enigmatic species: *Cynipencyrtus flavus* Ishii, a parasitoid of gall wasps (Cynipidae) (Ito & Hijii, 2000; Tachikawa, 1973, 1978), and *Cynipencyrtus indicus* Singh collected from *Quercus leucotrichophora* forest (Singh, 2008). Epichrysomallidae contains 19 genera (Burks et al., 2022) that are exclusively associated with figs (*Ficus*, Moraceae) (Rasplus et al., 2003). Melanosomellidae contains 31 genera (Burks et al., 2022), almost entirely from the Southern Hemisphere, associated with leaf or woody galls formed on various tree families, although the biology of most genera is unknown (Bouček, 1988). Tanaostigmatidae contains eight genera (LaSalle, 1987) that develop as primary gall formers, as inquilines within galls (LaSalle, 1987, 2005; van Noort & Copeland, 2020) or as seed feeders without gall formation (Lateef et al., 1985).

Fabricius (1804) described the first species of *Ormyrus* Westwood as *Chalcis nitidula*. Westwood (1832) described the genus *Ormyrus* within Chalcididae, with *O. punctiger* as the type species. Förster (1856) proposed the family Ormyridae (as Ormyroidae) for this genus, although *Ormyrus* has been treated subsequently in Ormyridae, Torymidae or Pteromalidae by different authors. In total, eight genera and a subgenus have been synonymized with *Ormyrus* (Noyes, 2019). *Siphonura* Nees and *Periglyphus* Boheman were synonymised by von Dalla Torre (1898). Förster (1860) artificially split *Ormyrus*, describing two further genera based on the number of anelli: *Monobaeus* Förster—one anellus, *Ormyrus*—two anelli, *Tribaeus* Förster—three anelli. Both additional genera, along with *Cyrtosoma* Perris, were subsequently synonymised with *Ormyrus* by Mayr (1904). The subgenus *Torymus* (*Chrysoideus*) De Stefani was synonymised by Risbec (1954). *Wania* Risbec was synonymised by Peck (1963). *Avrasyamyrus* Doganlar was synonymised by Hanson (1992). Currently, Ormyridae includes three genera—*Ormyrus* (144 species, worldwide), *Ormyrulus* Bouček (1 species, India and Oman) and the monotypic *Eubeckerella*

Narendran (Malaysia), which was described originally in Ormyridae but left unplaced to family by Burks et al. (2022).

Ormyrus occurs on all continents except for Antarctica and is the most diversified genus. Where biology is known, species of both *Ormyrus* and *Ormyrulus* are parasitoids of gall makers (Gomez et al., 2017). Most are parasitoids of Cynipidae on *Quercus* and other Fagaceae. Some are parasitoids of cynipids on Asteraceae, Lamiaceae, Papaveraceae and Rosaceae (Askew et al., 2006), or of chalcid wasps that develop in the syconia of fig trees (Moraceae: *Ficus*) (Bouček et al., 1981), or on other plant species (Askew & Blasco-Zumeta, 1998; Rasplus et al., 2011). Most non-hymenopterous host records are of Cecidomyiidae (Diptera) (Zerova & Seryogina, 2015). One of the most unusual hosts are weevil galls (Curculionidae: *Coccotorus chaoi* Chen) formed in twigs of *Celtis bungeana* Blume (Cannabaceae) in China (Yao & Yang, 2004). As parasitoids of insect pests, a few species are of economic importance. The indigenous European *Ormyrus pomaceus* (Geoffroy) (Gil-Tapetado et al., 2021) and the indigenous North American *O. labotus* (Cooper & Rieske, 2011) parasitize galls of *Dryocosmus kuriphilus* (Cynipidae), an introduced Chinese species that is a serious pest of chestnut trees. In India, *O. orientalis* Walker is a parasitoid of *Melanagromyza obtusa* (Malloch) (Agromyzidae), which is a pest of pigeon pea (*Cajanus cajan* (L.) Huth; Shanower et al., 1998), whereas *Ormyrulus gibbus* is a parasitoid of *Procontarinia matteiana* (Cecidomyiidae), a pest of mango (Bouček, 1986). The biology of the monotypic *Eubeckerella* remains unknown.

Recent next-generation molecular analyses, as well as morphological interpretation (Burks et al., 2022; Cruaud et al., 2024) supported relationships of the gall forming genera *Asparagobius* and *Hemadas* with the genera *Ormyrus* and *Ormyrulus*, which resulted in the transfer of these two genera from Ormocerinae (Pteromalidae) to Ormyridae by Burks et al. (2022). Unfortunately, the rare genus *Eubeckerella* was not included in Cruaud et al. (2024), which led Burks et al. (2022) to exclude the genus from Ormyridae and treat it as unplaced to family, although without explanation given for this reclassification. The Afrotropical *Asparagobius* is a gall former on *Asparagus* (Asparagaceae) (Mayr, 1905), whereas the Nearctic *Hemadas nubilipennis* (Ashmead) is a gall former on Blueberry, *Vaccinium angustifolium* Aiton (Ericaceae) (Shorthouse et al., 1986,

REDEFINING ORMYRIDAE

Systematic
Entomology

Royal
Entomological
Society

3

1990; West & Shorthouse, 1989). Moreover, as reported herein, an undescribed genus has been reared as a gall-maker on *Halleria* (Stilbaceae), a tree genus native to eastern and southern Africa and to Madagascar (Gibbs Russell et al., 1987).

This conceptual expansion of Ormyridae requires a formal taxonomic redefinition based on current molecular, morphological and biological knowledge. Here, we propose a phylogeny of Ormyridae with the inclusion of outgroup genera/species belonging to members of the 'Gall Clade' inferred from ultra-conserved elements (UCEs) and their flanking regions. Based on our molecular results and a comparative morphological character assessment, the classification of Ormyridae is revised from that of Burks et al. (2022). The aims of this paper are (1) to circumscribe Ormyridae including keys to subfamilies and genera and (2) to describe two new genera belonging to Ormyridae.

MATERIALS AND METHODS

Phylogenetic inference from UCE data

We inferred relationships among 15 species of Ormyridae (two species of which are new and described herein) belonging to four described genera (*Asparagobius*, *Hemadas*, *Ormyrus*, *Ormyrulus*) plus a new genus described herein, *Halleriaphagus*, **gen. nov.** Specimens of the rare, monotypic genus *Eubeckerella* were not available for inclusion in the molecular analyses. The two new species of *Ouma*, **gen. nov.** are only represented by their holotypes and hence specimens were not available for sequencing. Twenty-four species belonging to other families of Chalcidoidea, including members of the 'Gall Clade' sensu Cruaud et al. (2024) (Cynipencyrtidae, Epichrysomallidae, Melanosomellidae, Tanaostigmatidae) were also included (Table S1).

UCEs were obtained from previous publications (Blaimer et al., 2023; Cruaud et al., 2024; Rasplus et al., 2020; Rasplus et al., 2022), extracted from genomes (Bunnefeld et al., 2018) or captured de novo for the purpose of this study (Table S1) using the 2749 RNA probes designed by Faircloth et al. (2015). Lab protocol and pipeline for the analysis of raw reads are detailed in Cruaud et al. (2019). Briefly, adapter trimming and selection of high-quality paired reads was performed with Trimmomatic (Bolger et al., 2014); paired reads were merged with FLASH (Magoc & Salzberg, 2011) and demultiplexing was performed with a custom script. Assembly into contigs was performed with CAP3 (Huang & Madan, 1999) and contigs were aligned with Lastz (Harris, 2007) to the set of ca 1400 reference UCEs. Alignment of individual UCEs was performed with MAFFT (linsi option; Katoh & Standley, 2013). Alignment cleaning was performed with SEQ-TOOLS (Mirarab et al., 2014) by removing positions with more than 50% gaps and sequences with more than 25% gaps. Individual UCE trees were built with IQ-TREE 2.0.6 (Minh et al., 2020) with best fit models selected by ModelFinder (BIC criterion) (Kalyaanamoorthy et al., 2017). Only 'common substitution

models' were tested (i.e., JC, F81, K80, HKY, TN, TPM, TIM, TVM, SYM and GTR model families; Lie Markov and FreeRate models were not included in tests, −m TEST option in IQ-TREE). Two rounds of Treeshrink (Mai & Mirarab, 2018) were performed on individual UCE trees to remove abnormally long branches (b = 10 and realignment of loci between rounds with MAFFT). Only loci present in at least 70% of the samples were retained for phylogenetic analysis (N = 671).

Phylogenetic inference was performed on the concatenated UCEs using IQ-TREE either with or without partitioning of the data set. For the partitioned analysis, each UCE was first split into one core and two flanking regions using the Sliding-Window Site Characteristics (SWSC) method (Tagliacollo et al., 2018), and we used the best partitioning scheme inferred by PartitionFinder 2.1.1 (Lanfear et al., 2017) that joins core and flanking regions that share similar characteristics into subsets (model selection = AICc; algorithm = rclusterf; branch lengths linked). The starting tree set for all analyses using IQ-TREE was composed of 100 parsimony trees +1 BIONJ tree an improved version of the NJ algorithm (Gascuel, 1997) built from the sequences. However, only the 20 best initial trees (i.e., trees with the highest likelihoods) were retained for NNI (Nearest Neighbour Interchange) search (i.e., search with local tree rearrangement that swaps two subtrees across an internal branch) throughout the tree space to infer the final tree (default parameters in IQ-TREE). The best fit model for the unpartitioned data set was selected by ModelFinder and Free-Rate models with up to 10 categories of rates were included in tests. The best fit models for each data subsets of the partitioned data set were also selected by ModelFinder but, as detailed above, only common substitution models were tested. Statistical support of nodes was assessed with ultrafast bootstrap (UFBoot) with a minimum correlation coefficient of the split occurrence frequencies set to 0.99 to ensure that further tree search will not substantially alter the resulting support values and 1000 replicates of SH-aLRT tests (Guindon et al., 2010) to get two different sources of statistical support and improved confidence in results (IQ-TREE default parameters). Statistical support for a node was considered as strong when SH-aLRT ≥80% and UFboot ≥95% (cf IQ-TREE manual).

Phylogenetic inference was also performed using the tree reconciliation method implemented in ASTRAL-III (Zhang et al., 2018). Nodes in gene trees with UFBoot support lower than 90 were collapsed with the perl script AfterPhylo.pl (Zhu, 2014) before reconciliation and statistical support of nodes in the species tree was assessed with local posterior probabilities (local PP). Statistical support for a node was considered as strong when local PP >0.90.

Morphological assessment

Comparative morphological assessment of character states was undertaken across representatives of all genera previously placed

in the Ormyridae or considered to potentially belong to the family under our revised interpretation of taxon delimitation. Novel assessment of difficult to observe and previously overlooked characters, such as those associated with the underside of the head, configuration of the prepectus, and tarsal claw structure were focused on. Character states were scored and recorded in a matrix.

Imaging

Images acquired at the South African Museum, Cape Town (SAMC) used a Leica LAS 4.9 imaging system, comprising a Leica® Z16 microscope (using either a ×2 or ×5 objective) with a Leica DFC450 Camera and ×0.63 video objective attached; diffused lighting was achieved using a Leica LED5000 HDI dome; and the imaging process, using an automated Z-stepper, was managed using the Leica Application Suite V 4.9 software installed on a desktop computer. Images acquired at the National Research Institute for Agriculture, Food and the Environment (INRAE) used a Keyence digital microscope (VHX-5000 Camera colour CMOS and the VH-Z100UT lens). Images acquired at Alexandu Ioan Cuza University of Iaşi used a Leica DFC500 digital camera attached to a Leica M205A automated research stereomicroscope. All images presented in this paper, as well as supplementary images, are available on WaspWeb at www.waspweb.org (van Noort, 2023).

Lucid pathway and Lucid matrix keys were developed using Lucid Builder version 4.0.23. Character matrices were generated and edited using Microsoft Excel; matrices were then used as input into Lucid matrix key production (Penev et al., 2009). The online interactive keys were produced using Lucid meeting the requirements of publishing both static and dynamic interactive keys under an open access model (Penev et al., 2009). All keys were illustrated using high quality annotated images, highlighting diagnostic characters. The images are integrated into the key above each couplet resulting in a user-friendly output. This key format reduces the requirement of familiarity with morphological terminology associated with a particular taxonomic group, because the characters are visually illustrated making the keys usable by a wide range of end-users including ecologists and conservationists. Online identification keys are presented in two different formats on WaspWeb: traditional static dichotomous keys where a choice needs to be made at each key couplet to continue, which are also presented as an interactive Lucid pathway (dichotomous) key; and Lucid matrix keys where relevant states from multiple character features can be selected independently until identification is achieved. For more information concerning Lucid keys visit http://www.lucidcentral.org.

Morphological terminology mostly follows the Hymenoptera Anatomy Ontology (HAO: http://portal.hymao.org) (Yoder et al., 2010) and Gibson (1997) for structural terms, and Harris (1979) for sculpture terms. Classification of vegetation (habitat association) follows Mucina and Ruthaford (2006).

Abbreviations and terms used in text and figures

Ocelli

LOL: Lateral ocellar line, shortest distance between margins of median and lateral ocelli.
OOL: Ocular ocellar line, shortest distance between inner orbit and outer margin of posterior ocellus.
POL: Posterior ocellar line, shortest distance between inner margins of posterior ocelli.

Back of head

hyc: hypostomal carina—the dorsal extensions of which flank the lower tentorial bridge.
ltb: lower tentorial bridge—a potentially composite but partially tentorial structure extending from the postocciput to the hypostoma.
lts: lower tentorial sulcus—a line or sulcus extending ventrally from the secondary posterior tentorial pit, separating the lower tentorial bridge from the postgena.
occ: occipital carina—occurs dorsal to the occipital foramen and ventro–medially to the vertex and genae, crossing or potentially helping delimit the occiput.
pom: postoral microtrichia—a variably shaped median strip present on the lower tentorial bridge.
psg: postgena—the ventral, posterior surface of the head below the dorsal margin of the occipital foramen.
ptp: posterior tentorial pit—primary pits, occurring near the mid-height constriction of the foramen magnum.
sptp: secondary posterior tentorial pit—situated about midway between the primary posterior tentorial pit and the hypostoma.

Structures of mesosoma around prepectus

mpl: mesopleuron.
msc: mesoscutum.
pre: prepectus—an intersegmental sclerite that is visible usually as a more or less triangular sclerite on either side of the thorax between the pronotum and mesopleuron.
pro: pronotum.
tgl: tegula.

Abbreviations of depositories

CBGP: Centre de Biologie pour la Gestion des Populations (Curator: Emmanuelle Artige).
ICIPE: International Centre of Insect Physiology and Ecology, Nairobi (Curator: Robert Copeland).
NHMUK: Natural History Museum, London (Curator: Natalie Dale-Skey).
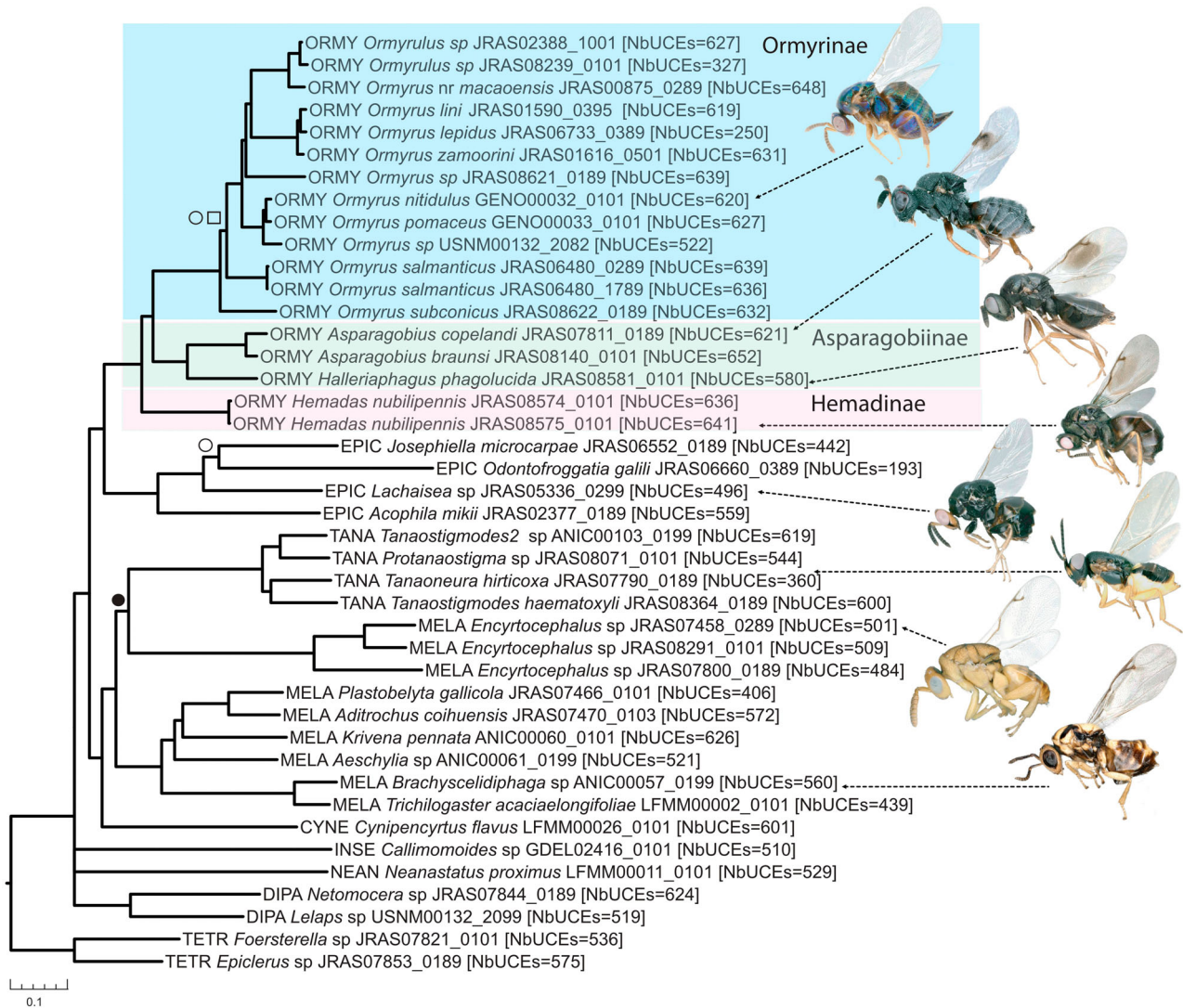NMPC: Natural History Museum, Prague (Curator: Tomáš Hovorka).

FIGURE 1 Phylogenetic relationships. The IQ-TREE tree (unpartitioned data set) is used as template. Unsupported nodes (IQ-TREE SH-aLRT <80 and/or UFBoot <95) are collapsed. Collapsed nodes are not supported in the IQ-TREE tree obtained from the partitioned data set and the ASTRAL tree (local PP <0.9) either. Abbreviations for family names in tip labels are as follows: CYNE, Cynipencyrtidae; DIPA, Diparidae; EPIC, Epichrysomallidae; INSE, *Incertae sedis*; MELA, Melanosomellidae; NEAN, Neanastatidae; ORMY, Ormyridae; TANA, Tanaostigmatidae; TETR, Tetracampidae. The number of ultra-conserved elements (UCEs) analysed for each sample is given in brackets. Nodes were highly supported (IQ-TREE SH-aLRT ≥80/UFBoot ≥95; ASTRAL local PP ≥0.9) unless specified with symbols. White squares indicate nodes that were observed but not supported in the alternative IQ-TREE tree obtained from the partitioned data set; white circles indicate nodes that were observed but not supported in the ASTRAL tree; black circles indicate nodes that were not observed in the ASTRAL tree. Complete IQ-TREE and ASTRAL trees are available in Figure S1. Photos (©J.-Y. Rasplus) are illustrations of the genera that arrows point to. Local PP = local posterior probabilities.

SAMC: South African Museum, Iziko Museums of South Africa, Cape Town (Curator: Simon van Noort).

RESULTS

Phylogenetic relationships

Ormyridae was recovered as monophyletic with strong support in all analyses (Figure 1 and Figure S1–671 UCEs and 341,568 bp analysed). Relationships among ingroup species were identical in the IQ-TREE trees (with and without partitioning) and the ASTRAL tree, with the genus *Hemadas* consistently recovered as sister to all other ormyrids with strong support. *Halleriaphagus*, **gen. nov**. was sister to *Asparagobius* with strong support in all topologies. *Ormyrulus* consistently made *Ormyrus* paraphyletic. A few unsupported differences were observed between the IQ-TREE and ASTRAL trees only for the relationships inferred among outgroup species (position of *Neanastatus*, *Callimomoides* and *Encyrtocephalus*). Besides the description of five new species and the new genera *Halleriaphagus*, **gen. nov**. and *Ouma*, **gen. nov**., as detailed below, these results together with current morphological (in particular, the structure of the posterior of the head, the
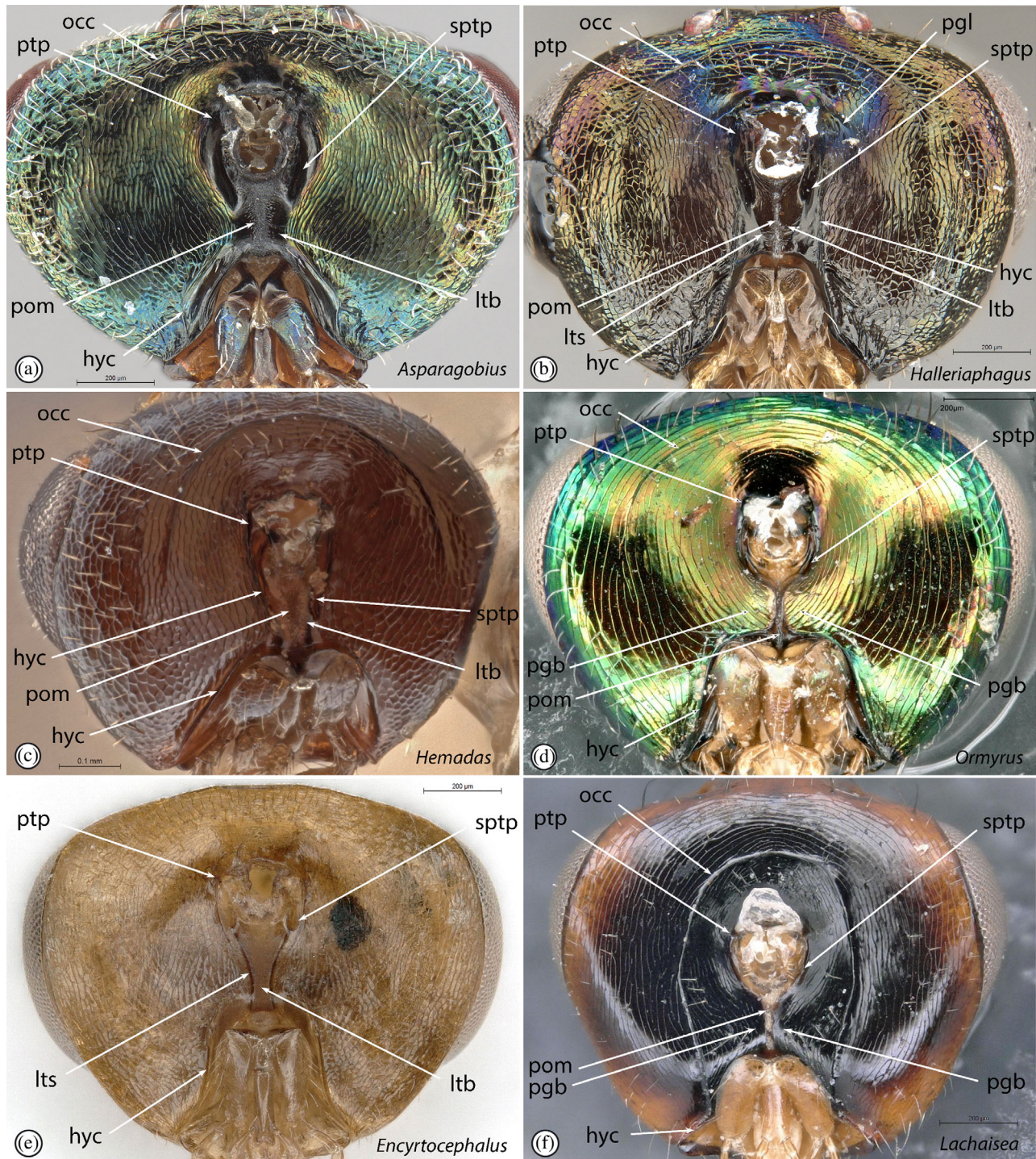
FIGURE 2 Structural configuration of the posterior of the head of four Ormyridae genera (a–d) and two related gall making genera in the families Melanosomellidae (e) and Epichrysomallidae (f). (a) *Asparagobius braunsi*; (b) *Halleriaphagus phagolucida*; (c) *Hemadas nubilipennis*; (d) *Ormyrus* sp.; (e) *Encyrtocephalus* sp.; (f) *Lachaisea* sp. See materials and methods for explanation of abbreviations used here.

prepectal lateral panel and tarsal claw configuration) and biological knowledge led us to (1) support the transfer of *Asparagobius* and *Hemadas* to Ormyridae (implemented by Burks et al., 2022), (2) synonymize *Ormyrulus* with *Ormyrus*, **syn. nov.**; (3) erect two new subfamilies for Ormyridae: Asparagobiinae, **subfam. nov.,** and Hemadinae, **subfam. nov.;** (4) reestablish *Eubeckerella* within Ormyridae and (5) classify *Eubeckerella*, *Ormyrus* and *Ouma* within Ormyrinae.

Morphological assessment

The character states scored as a result of the comparative morphological assessment of six genera (*Asparagobius*, *Eubeckerella*, *Halleriaphagus*, *Hemadas*, *Ormyrus* and *Ouma*) considered to belong to the Ormyridae are presented as a matrix in Table S2. A comparative illustration of characters associated with the back of the head is

REDEFINING ORMYRIDAE

Systematic
Entomology

Royal
Entomological
Society

7

FIGURE 3 Relative structural configuration of the prepectus (pre) in the six recognized Ormyridae genera. (a) *Asparagobius bouceki*; (b) *Halleriaphagus phagolucida*; (c) *Hemadas nubilipennis*; (d) *Eubeckerella malaica*; (e) *Ormyrus subconicus*; (f) *Ouma emazantsi*. See Materials and Methods for explanation of abbreviations used here.

presented in Figure 2, of those characters associated with the configuration of the prepectus in Figure 3, and representative images of the various tarsal claw structures are presented in the respective species plates. Based on the comparative morphological assessment, the relative structural configuration of the lateral panel of the prepectus with respect to the surrounding sclerites is proposed as a morphological synapomorphy for the newly defined Ormyridae. In all six genera the prepectus is foliaceous, loose relative to surrounding sclerites, overlapped by the posterior margin of the pronotum which lies in close approximation to the surface of the lateral panel, and the prepectal lateral panel itself overlies the base of the tegula; the surface of the lateral panel of the prepectus is flat and lacking any internal groves or elevation; the lateral panel is dorsally somewhat convex, not straight; mesothoracic spiracle is clearly visible externally at the junction of the pronotum, mesonotum and the lateral panel of prepectus. This is a structural configuration,

which is unique within the Chalcidoidea (Figure 3). Specimens of the two rare genera, *Eubeckerella* and *Ouma*, were not available for dissection to observe the structure of the posterior surface of the head, which needs to be detached from the body for this purpose. The remaining four genera showed overall similarities in character states associated with the posterior head surface, including a dorsally complete occipital carina (occ) that fades laterally on both sides not reaching the hypostomal carina (Figure 2a–d). The occipital carina is complete, reaching the hypostomal carina in the sister family Epichrysomallidae (Figure 2f), suggesting that the lateral reduction of the carina is a loss in Ormyridae. The lower tentorial bridge (ltb) is visible in three of the genera (*Asparagobius*, *Halleriaphagus*, *Hemadas*) with the median strip of the pom present (Figure 2a–c). The pom strip is also present in *Ormyrus*, but here the post-genal bridge has closed over the lower tentorial bridge obscuring this structure laterally, suggesting that this is a derived condition in *Ormyrus* supported by the derived Ormyrinae clade recovered in the molecular phylogenetic analyses. The exposed lower tentorial bridge is also present in another 'Gall Clade' family (Melanosomellidae) (Figure 2e), but here the occipital carina and postoral microtrichia strip are absent. The shared configuration of the character states across the four examined genera of the posterior head surface were not sufficiently unique within the Chalcidoidea to be proposed as additional synapomorphic characters defining the Ormyridae. Other potential synapomorphies include the mesotrochantinal plate in front of the mid coxae which is usually sclerotized with backward pointing lateral lobes (Figure 24e,f), whereas this area is usually membranous in the other families of the 'Gall Clade'. Further potential synapomorphies include the large metacoxal foramen, which has a diameter about twice that of the metasomal foramen (Figure 24e,f); the hind coxal foramina being in close apposition, their separation less than the diameter of the metasomal foramen (Figure 24e,f); and the very narrow sclerite between the metacoxal and metasomal foramen (Figure 24e,f).

Taxonomic revision of Ormyridae

Thorough (re)description of all genera and the new subfamilies and keys to species are provided in this section.

Ormyridae Förster, 1856.

Ormyroidae Förster, 1856: 19, 22, 24.
Ormyrides Förster, 1856. In: Thomson, 1876: 100.
Ormyrinae Förster, 1856. In: Ashmead, 1904: 245.
Ormyrinae Förster, 1856. In: Girault, 1915: 309.
Ormyrinae Förster, 1856. In: Bouček, 1988: 155.
Ormyridae Förster, 1856. In: Doganlar, 1991: 3.

Diagnosis. Antenna usually with 12 apparent flagellomeres (Figure 19c), including very small fourth clavomere (terminal button), the latter sometimes partly to completely fused with third clavomere. Eyes not ventrally divergent (Figure 19b). Clypeus bilobed (Figure 21c), or at least broadly emarginate to straight medially (Figure 36d), without transverse subapical groove.

Labrum hidden behind clypeus, flexible, subrectangular with row of marginal setae. Mandibles with 2 teeth, plus a molar truncation (Figure 21c). Subforaminal bridge with postgenal lobe separating secondary posterior tentorial pit from hypostoma and restricting it to the vicinity of occipital foramen (Figure 2a–d); postgenal bridge present or separated and therefore lower tentorial bridge reaching or not reaching hypostoma (Figure 2a–d); postgenal lamina usually absent; hypostomal carina usually (but not always) convergent; occipital carina present, and usually very visible, although sometimes ventrolateral edges extending only to the dorsal margin of hypostomal foramen (Figure 2a–d). Prepectus foliaceous, largely hidden beneath the posterior–lateral margin of the pronotum with dorsal and posterior prepectal margins overlapping the mesoscutal margin as well as the base of the tegula (Figure 3). Axillae at least slightly advanced (Figure 19d). Mesoscutellum with frenum indicated at least laterally by apparent change in sculpture or only by mesoscutellar arm; without axillular sulcus, and with flap-like marginal rim extending at least over metascutellum (Figure 19d). Mesopleuron without an expanded acropleuron; posterior margin of mesepimeron extending over anterior margin of metapleuron (Figure 32c); mesotrochantinal plate inflected dorsally between mesocoxal fossae, with dorsal margin of plate broadly contiguous with lower metepisternum (Figure 24e,f) or narrowly separated from it by membrane (Figure 39b). Metacoxal foramina large, distance between them less than breadth of propodeal foramen; diameter of metacoxal foramen about $1.5\times$ as broad as propodeal foramen diameter (Figure 24e,f). All legs with 5 tarsomeres; protibial spur stout and curved and bifurcate; basitarsal comb longitudinal. Fore wing stigmal vein not at right angle with anterior margin of fore wing (Figure 18e). Gaster with Gt_7 and Gt_8 fused into syntergum and therefore without separate epipygium (Gt_8), convex (Figure 19f) or (more frequently) strongly sclerotized and carapace-like (Figure 42d).

Morphology overview. Ormyridae can generally be defined as robust chalcids that vary in size from 1 to 7 mm (Figure 41a) and that have enlarged metacoxae that are broadly connected to the mesosoma (Figure 41e); they almost always also have a conspicuous occipital carina (Figure 2a–d) and often also a very convex mesosoma and strongly sclerotized gaster (dorsally conspicuously sculptured in the case of most of Ormyrinae), and usually are metallic blue or green, sometimes metallic bronze or violet, although occasionally black (e.g., Figures 18, 22, 28, 30, 36, 41 and 45). The lateral panel of the prepectus is foliaceous and is partly hidden beneath the posterior–lateral flap of the pronotum (Figure 3). The dorsal margin of the prepectus overlaps the mesoscutal margin as well as the tegula, reaching slightly beyond the base of the tegula (Figure 3a–f) and is tightly overlapped by the posterior margin of the lateral pronotum. The mesotrochantinal plate in front of the mid coxae is usually sclerotized with backward pointing lateral lobes (Figure 24e,f). The hind coxal foramen is large, with a diameter about twice that of the metasomal foramen (Figure 24e,f). The distance between the hind coxal foramina is less than the diameter of the metasomal foramen (Figure 24e,f). A narrow sclerite is present between the metacoxal and metasomal foramen (Figure 24e,f).

REDEFINING ORMYRIDAE

Systematic
Entomology

Royal
Entomological
Society

9

The head in frontal view is generally much wider than high. The clypeal margin is slightly (Figure 39a) to conspicuously protruding (Figure 21c) and usually bilobed or emarginate, though in *Hemadas*, it is almost straight (Figure 36d). The eyes of most Ormyridae have normal dimensions, at most three or four times as high as the length of the malar space, except in *Eubeckerella malaica* where they are unusually large, about seven times as high as the length of the malar space (Figure 40a). The antennal toruli are situated much higher than the lower eye margin; the number of anelli to funiculars can be 1:7 (*Asparagobius*, *Eubeckerella*, some *Ormyrus*), 2:6 (*Halleriaphagus*, *Hemadas*, some *Ormyrus*, *Ouma*) or even 3:5 (some *Ormyrus*). In Ormyrinae, the postgenal bridge is closed and the postgenae are separated only by a narrow strip of postoral microtrichia, whereas in Asparagobiinae and Hemadinae, the postgenal bridge is open and the postgenae are separated by the lower tentorial bridge (Figure 2a–d).

The mesosoma is distinctly arched dorsally (Figure 41e). The notauli are complete, but usually shallow and only distinctly represented anteriorly (Figure 41c). The mesoscutellum lacks an axillular or frenal groove, but the frenum is indicated at least laterally by a change in sculpture or by the mesoscutellar arms (Figure 41f). The propodeum is usually short and devoid of carinae, except for one or several median carinae. In *Asparagobius*, *Hemadas* and *Ormyrus*, the median part of the propodeum is almost vertical and has the mesoscutellum projecting over it (Figure 41e), whereas in other genera, the propodeum is more or less inclined. The metacoxa is large or very large (usually about twice the procoxal length) (Figure 41e) and connected to the mesosoma through a broad foramen (Figure 24f). The ventral margin of the metapleuron is obliquely angled and in lateral view the ventral margin of the callus slightly overlaps the dorsal angle of the metacoxa and forms an obtuse angle with the posterior margin of the metapleuron (Figure 41c). In *Ormyrus*, the two metatibial spurs are stout and curved apically. The tarsal claws have either a rudimentary basal hump in Hemadinae (Figure 38f) or a large basal projection that may be cleft in Asparagobiinae (Figure 23e) and most Ormyrinae. The venation of the fore wing is generally characterized by a short stigmal vein (Figure 31f), except in *Hemadas* (Figure 37e). Ormyrinae have a very long marginal vein, which is at least 3.5× the length of the postmarginal vein (Figure 42g), whereas Asparagobiinae (Figure 22f) and Hemadinae (Figure 37e) have a shorter marginal vein, at most 2.5× the length of the postmarginal vein.

The gaster is sessile and the gastral tergites exhibit a wide range of sculpture types, from almost smooth in *Eubeckerella*, *Halleriaphagus* and *Ouma* (Figure 45d) to having deep foveae (pits) in *Ormyrus* (Figure 42d), with intermediate sculpture in *Asparagobius* (Figure 22e); however, most tergites are at least weakly sculptured distally or/and laterally. Species of *Ormyrus* have the gaster strongly sclerotized and heavily sculptured, usually with transverse rows of large pits basally on the middle tergites, this foveate base is generally separated from the apical part of the tergite by a crenulate border bearing strong, bristle-like setae. Cerci are button-like in *Ormyrus* (Figure 42e), whereas they are peg-like in *Asparagobius*, *Eubeckerella*, *Halleriaphagus*, *Hemadas* and *Ouma* (Figure 24d).

Biology. Ormyridae are associated with plant galls, either as gall formers or as parasitoids of gall formers. Species of *Asparagobius* form galls on *Asparagus* (Asparagaceae) (Figures 25–27), whereas the only known species of *Hemadas* produces galls on *Vaccinium* (Ericaceae). The monotypical *Halleriaphagus phagolucida* was reared from galls on *Halleria lucida* L. and *Halleria elliptica* L. (Stilbaceae) (Figures 34 and 35). Species of *Ormyrus* are parasitoids of gall formers. A summary of the literature listing host associations of *Ormyrus* as well as detailed original observations on the morphology and biology of *Ormyrus* larvae were provided by Gomez et al. (2017). The biology of *Eubeckerella* and *Ouma* is unknown.

Distribution. Worldwide. Ormyridae is a cosmopolitan family, although *Hemadas nubilipennis* (Hemadinae) is known only from the Nearctic region and Asparagobiinae only from the Afrotropical region. Species of Ormyrinae occur on all continents except Antarctica, and are known even from several Pacific islands, including the Solomon Islands, New Caledonia, Vanuatu (New Hebrides) and Samoa, but not New Zealand (Noyes, 2019; Hanson, unpubl. data). *Ormyrus* is cosmopolitan, although there are very few records from South America. Specimens of *Ormyrus* have been reared from oak galls in Colombia (Hanson, unpubl. data), but only two specimens are known from the rest of the continent, both from western Brazil— *O. brasiliensis* from Chapada dos Guimarães (Mato Grosso), and an undetermined species from Corumbá (Mato Grosso do Sul) (Shimbori et al., 2017). *Eubeckerella* is so far restricted to Malaysia, whereas *Ouma* is Afrotropical.

Proposed reclassification of Ormyridae

Asparagobiinae van Noort, Burks, Mitroiu and Rasplus, **subfam. nov.**

    Asparagobius Mayr, 1905.

        Asparagobius bouceki van Noort, **sp. nov.**

        Asparagobius braunsi Mayr, 1905.

        Asparagobius copelandi Rasplus and van Noort, **sp. nov.**

    Halleriaphagus van Noort and Burks, **gen. nov.**

        Halleriaphagus phagolucida van Noort and Burks, **sp. nov.**

Hemadinae van Noort, Burks, Mitroiu and Rasplus, **subfam. nov.**

    Hemadas Crawford, 1909.

        Hemadas nubilipennis (Ashmead, 1887).

Ormyrinae Förster, 1856.

    Eubeckerella Narendran, 1999.

        Eubeckerella malaica Narendran, 1999.

    Ormyrus Westwood, 1832.

        Ormyrus 144 species [for full list see UCDW, 2023].

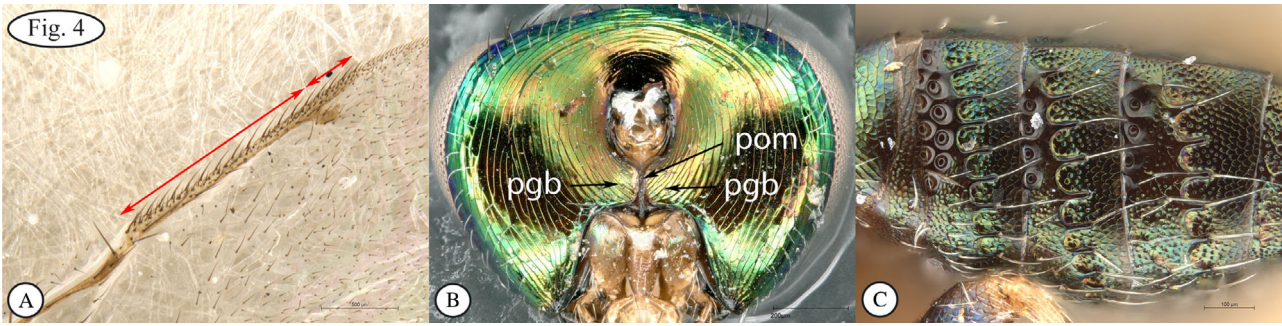   *Ormyrus gibbus* (Bouček, 1986), **comb. nov.**

    Ouma Mitroiu, **gen. nov.**

        Ouma daleskeyae Mitroiu, **sp. nov.**

        Ouma emazantsi Mitroiu, **sp. nov.**

Key to subfamilies and genera of Ormyridae

1. Marginal vein long, at least 3.5× length of postmarginal vein (Fig. 4A); postgenal bridge closed (pgb), postgenae separated only by narrow strip of postoral microtrichia (pom) (Fig. 4B); gastral tergites often with transverse rows of foveae and crenulations (Fig. 4C) .... 3 **ORMYRINAE**

- Marginal vein shorter, at most 2.5× length of postmarginal vein (Fig. 5a); postgenal bridge open, postgenae separated by lower tentorial bridge (ltb) (Fig. 5b); gastral tergites rarely with weak crenulations present laterally (Fig. 5c) 2

2. Tarsal claws with large basal projection that is cleft (Fig. 6A); uncus small, hardly protruding (Fig. 6B); clypeal margin strongly protruding (Fig. 6C) .... 5 **ASPARAGOBIINAE**
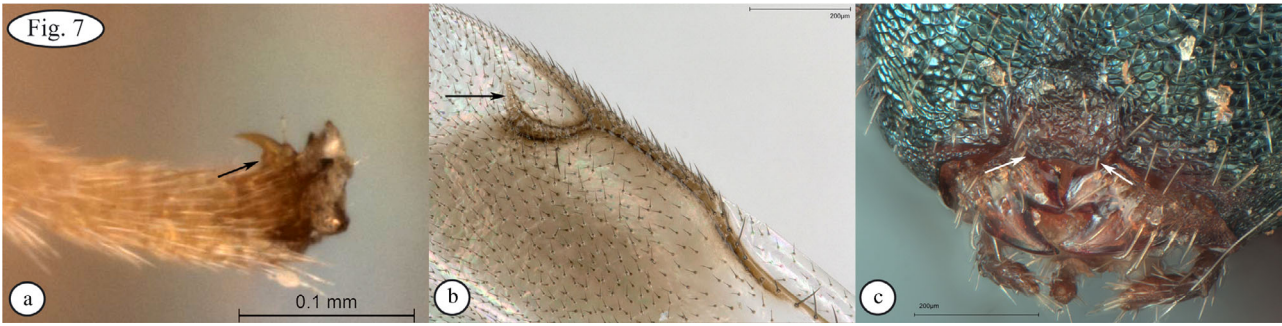
Fig. 7

- Tarsal claws simple, with rudimentary basal hump (Fig. 7a); uncus long, half-length of stigmal length (Fig. 7b); clypeal margi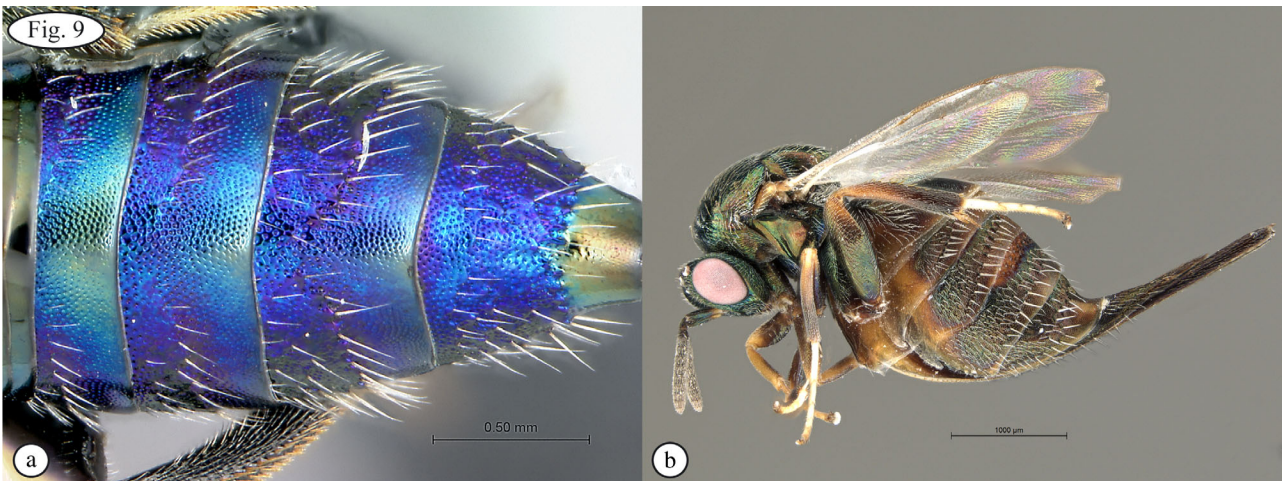n weakly protruding (Fig. 7c) .... **HEMADINAE** (*Hemadas*)

Fig. 8

3. Gastral tergites, except the first, shallowly and evenly punctulate-reticulate (Figs 8A,B) 4

Fig. 9

- Gastral tergites, except the first, strongly sculptured, often with transverse rows of larger pits on the tergites and strong setation (Figs 9a,b) .... *Ormyrus*
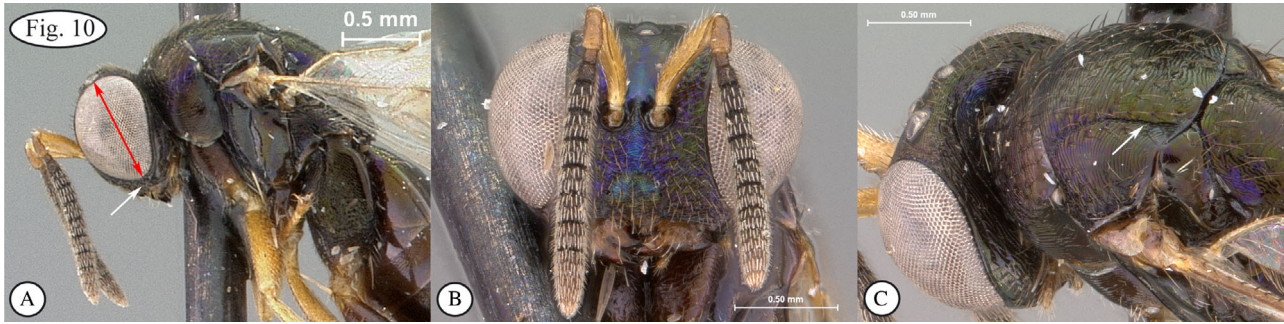
4. Eyes very large, hence malar space very short (Fig. 10A); face mainly rugose-striate (Fig. 10B); notauli deep in posterior part (Fig. 10C); antennal formula 11173 (Fig. 10B); fore wing with diffuse median infumation .... *Eubeckerella*
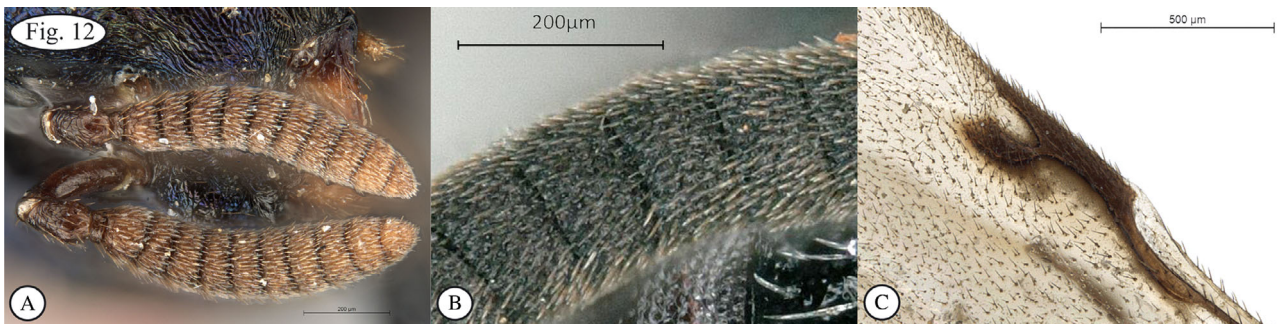

- Eyes normal, malar space much longer (Fig. 11a); face mainly reticulate (Figs 11a,b); notauli shallow to almost indistinct at least in posterior part (Fig. 11c); antennal formula 11263 (Fig. 11b); fore wing hyaline .... *Ouma*

5. Antennal formula 11174 (Fig. 12A); multiporous plate sensilla small and numerous, present in multiple (up to 6) interspersed rows on each flagellomere (Fig. 12B); stigmal vein parallel to postmarginal vein, thickened, cleaver-shaped (Fig. 12C) .... *Asparagobius*

– Antennal formula 11264 (Fig. 13a); multiporous plate sensilla large, present in 1 to 2 rows on each flagellomere (Fig. 13b); stigmal vein at about an 80-degree angle to postmarginal, club-shaped (Fig. 13c) .... *Halleriaphagus*

Asparagobiinae van Noort, Burks, Mitroiu and Rasplus, subfam. nov.

LSID   urn:lsid:zoobank.org:act:5712E3D6-DA78-44A1-83F5-F6D13BD9F7BE.

Type genus: *Asparagobius* Mayr, 1905.

Diagnosis. Head with clypeal margin strongly protruding (Figure 21c), postgenal bridge open with postgenae separated by lower tentorial bridge (Figure 2a) and postgenal lamina present (Figure 31a) or absent (Figure 2a); antennal formula 11264 (Figure 31d) or 11174 (Figure 21b); flagellum with multiporous plate sensilla either large, and in one to two rows on each flagellomere (Figure 31d), or small and numerous, present in up to six interspersed rows on each flagellomere (Figure 21b); fore wing with marginal vein at most 2.5× length of postmarginal vein, stigmal vein either at about an 80 degree angle to postmarginal vein and club-shaped (Figure 31f), or parallel to postmarginal vein and thickened, cleaver-shaped (Figure 18e) and with uncus large or small; tarsal claws with large basal projection that is cleft (Figure 23d); gastral tergites at most with weak crenulations.

Distribution. Afrotropical region.

*Asparagobius* Mayr, 1905 (Figures 14–29).

Asparagobius Mayr, 1905. **Type species**: *Asparagobius braunsi* Mayr, 1905.

Diagnosis. Antennal formula 11174 (Figures 19c and 28a); multiporous plate sensilla small, numerous, present in up to 6 interspersed rows on each flagellomere; occipital carina present, very slightly curved, with two medial angularities in line with lateral ocelli (Figure 2a); postgenal lamina absent (Figure 2a); tarsal claw with large basal projection that is cleft (Figure 23d–f); stigmal vein parallel to postmarginal vein, thickened, cleaver-shaped (Figure 18e).

Biology. Phytophagous gall formers on *Asparagus* species (Asparagaceae) (Figures 25–27).

Distribution. Kenya, South Africa.

Key to *Asparagobius* species
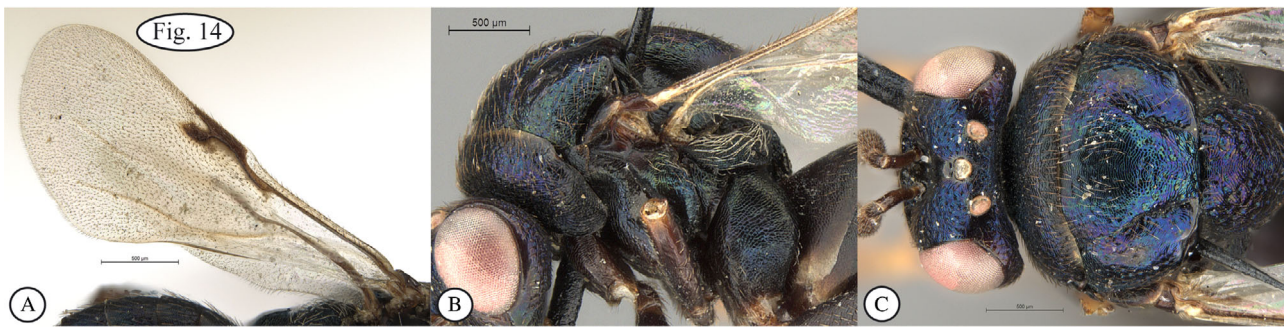
1. Fore wing hyaline (Fig. 14A); metapleuron triangular, acutely angled dorsally (Fig. 14B); integument with metallic blue iridescence (Figs 14B,C) ....…… *Asparagobius bouceki* van Noort, sp. nov.

– Fore wing with dark infuscate region (Fig. 15a); metapleuron rhomboidal, the dorsal margin truncate (Figs 15b,c); integument metallic greenish-bronze (Fig. 15b) or matt black (Fig. 15c) ....…… 2
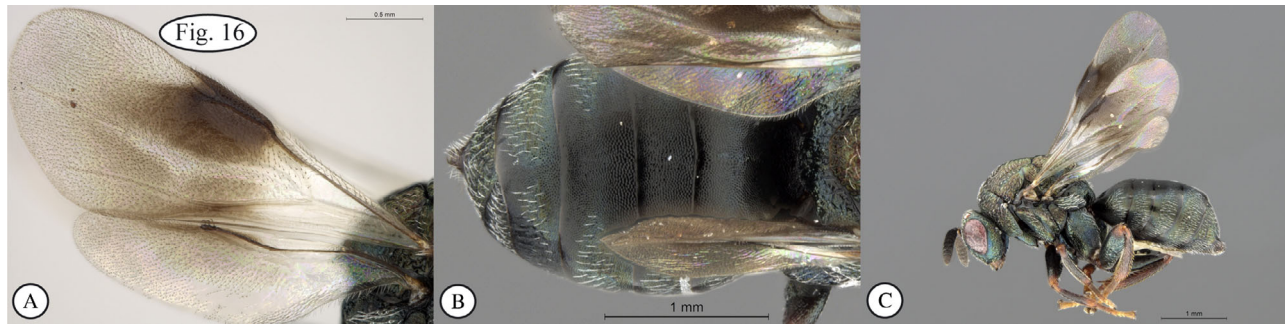
2. Fore wing with extensive infuscation (Fig. 16A); marginal vein twice length of stigmal vein (Fig. 16A); gaster sparsely setose (Figs 16B,C); body metallic greenish-bronze (Fig. 16C) .... *Asparagobius braunsi* Mayr

– Fore wing with infuscation restricted to smaller region (Fig. 17a); marginal and stigmal veins equivalent in length (Fig. 17a); gaster more extensively setose (Figs 17b,c); body matt black (Fig. 17c) .... *Asparagobius copelandi* Rasplus and van Noort, sp. nov.

Asparagobius bouceki van Noort, sp. nov. (Figures 18–21).
LSID urn:lsid:zoobank.org:act:6A38C173-687C-4860-9F5A-AF24B6 DF797D.

Holotype. ♀: SOUTH AFRICA, [*Northern Cape*] Kamieskroon—Springbok, Thorne, 1939, larvae of this wasp (Callimomidae) or Torymidae make puff-like galls on Asparagus, (with two galls on separate pins both labelled 'Gall from Asparagus no 1'), IMAGED WaspWeb, LAS 4.9, SAMC 2022, SAM-HYM-P009892. Deposited in SAMC.

Paratypes. SOUTH AFRICA, [*Northern Cape*] 1♀: Naib, Bushmanland, Btw Springbok and Pella, Mus. staff., Oct 1939, SAM-HYM-P009893 (SAMC). 1♂ : Bulhoek, Klaver-Clanwilliam, Mus. Exped., Oct 1950, SAM-HYM-P013117 (SAMC). [*Western Cape*] 4♀, Cape Town, SA Museum, museum staff, May 1940, SAM-HYM-P013118 (SAMC); 1♀: Malmsberg [=Malmesbury], Cei Capetown, 7 Novbr. 1925, coll. Bolloni, Asp affinis Bolloni (NMPC); 2♀, 2♂, Malmesbury, 7 Nov. 1925, R. Nel (NHMUK); 2 M, Malmesbury, 4. Nov. 1925, R. Nel (NHMUK); 2♀ (NHMUK), 1♂ (NMPC), Malmesbury, 12 Nov 1925, R. Nel; 3 F, 1♂ Stellenbosch, November 1925, R.I. Nel (2♀ IMAGED WaspWeb LAS 4.9 SAMC 2020) (NMPC).

Diagnosis. Metapleuron triangular, acutely angled dorsally (Figure 18d); fore wing hyaline (Figure 18e); integument with metallic blue lustre (Figure 18a).

Differential diagnosis. The other two species have a rhomboidal metapleuron, the fore wing with a dark infuscate patch below venation and are metallic green–bronze (*A. braunsi*) or matt black (*A. copelandi*) in body colour.

Etymology. Named in recognition of the extraordinary efforts of Zdeněk Bouček with respect to establishing sense in Chalcidoidea taxonomy. Noun in genitive case.

Biology. Reared from galls on *Asparagus*.

Distribution. South Africa.

Comments. There is some uncertainty as to whether the specimens currently present in the Natural History Museum in Prague (NMPC) should actually be in the Natural History Museum in London (NHMUK) (John Noyes pers. comm.).

Description. Body length 3.5–4.0 mm.

Colour. Body almost entirely metallic blue–black, with some purple lustre, becoming yellow–brown on areas of legs and flagellum (Figures 18 and 19); wings hyaline, venation dark brown; eyes and ocelli pink–white; setae mostly brown, white in some areas (mesepimeron, propodeum).

FIGURE 18 *Asparagobius bouceki* van Noort, sp. nov., holotype ♀ SAM-HYM-P009892 (SAMC). (a) habitus, lateral view; (b) habitus, dorsal view; (c) head, anterior view; (d) head, mesosoma, lateral view; (e) wings; (f) data labels.

Head. Antenna with scape 3.5× as long as broad, extending almost two thirds of distance to median ocellus (Figure 19a); pedicel 1.5× as long as $fl_1 + fl_2$, with scattered long setae; flagellum length 0.8× head height, with a transverse anellus, seven funiculars and three clavomeres; funicle broad at fl_1 and remaining funiculars of same width; flagellum tapering gradually through clava; fl_3 2.2× broader than long, with

remaining funiculars of equivalent dimensions; clava undifferentiated in structure from funiculars (Figure 19c); all funiclars and clavomeres with many small, densely packed multiporous plate sensilla in three interspersed rows (Figure 19c). Mandible stout, with two strong, acute teeth apically (inner tooth shorter than apical tooth) and a short, blunt, third tooth basally (Figure 19b). Head sculpture imbricate, and with

FIGURE 19 *Asparagobius bouceki* van Noort, sp. nov., paratype ♀ (NMPC). (a) head, anterior view; (b) head, anterior view; (c) antennae, dorsal view; (d) mesoscutellum, propodeum, dorsal view; (e) head and mesosoma, dorsal view; (f) gaster, dorsal view.

scattered setae (Figure 19b). Interantennal process weak. Toruli separated from each other by torulus diameter (Figure 19b). Eyes with small, scattered white setae; interocular distance 1.5× eye height; inner eye margins subparallel to each other, slightly converging ventrally; malar space 0.4× eye height (Figure 19b). Ocellar triangle raised. POL:OOL: LOL = 16:7:6 (Figure 19e). Antennal scrobe shallow and

broad, with rounded margins, narrowly and shallowly extending to median ocellus. Anterior tentorial pits evident as slight depressions. Clypeus 1.5× wider than high, slightly concave overall; bilobed clypeal margin with shallow, obtuse, medial triangular indentation (Figure 19b); dorsal clypeal sulcus angularly bell-shaped, with faint sulci extending to toruli. Labrum hidden. Occipital carina present dorsally, gently curved, but medially

FIGURE 20 *Asparagobius bouceki* van Noort, sp. nov., paratype ♀ (NMPC). (a) head, posterior view; (b) head, posterior–ventral view; (c) gastral tergites 7 and 8, posterior–dorsal view; (d) gastral terminal tergites, ovipositor, ventral view; (e) metatarsal claws, axial view (inset: data labels); (f) metatarsal claws, distal view.

humped; postgenal lamina absent (Figure 20a). Subforaminal bridge with postgenae narrowly separated, lower tentorial bridge slightly sunken; posterior tentorial pits situated lateral of upper foramen magnum; secondary posterior tentorial pits deep and long, positioned lateral to lower foramen magnum and dorsal half of tentorial bridge; hypostomal carinae hardly evident, not

extending to posterior tentorial pits, fading two-thirds up oral fossa (Figure 20a). Pom present along a broad median area encompassing width of lower tentorial bridge (Figure 20a).

Mesosoma. Pronotum, mesoscutum and mesoscutellum with scattered short setae (Figures 18d and 19e). Mesoscutum twice as broad as long, equal in length to mesoscutellum; mesoscutal lobes
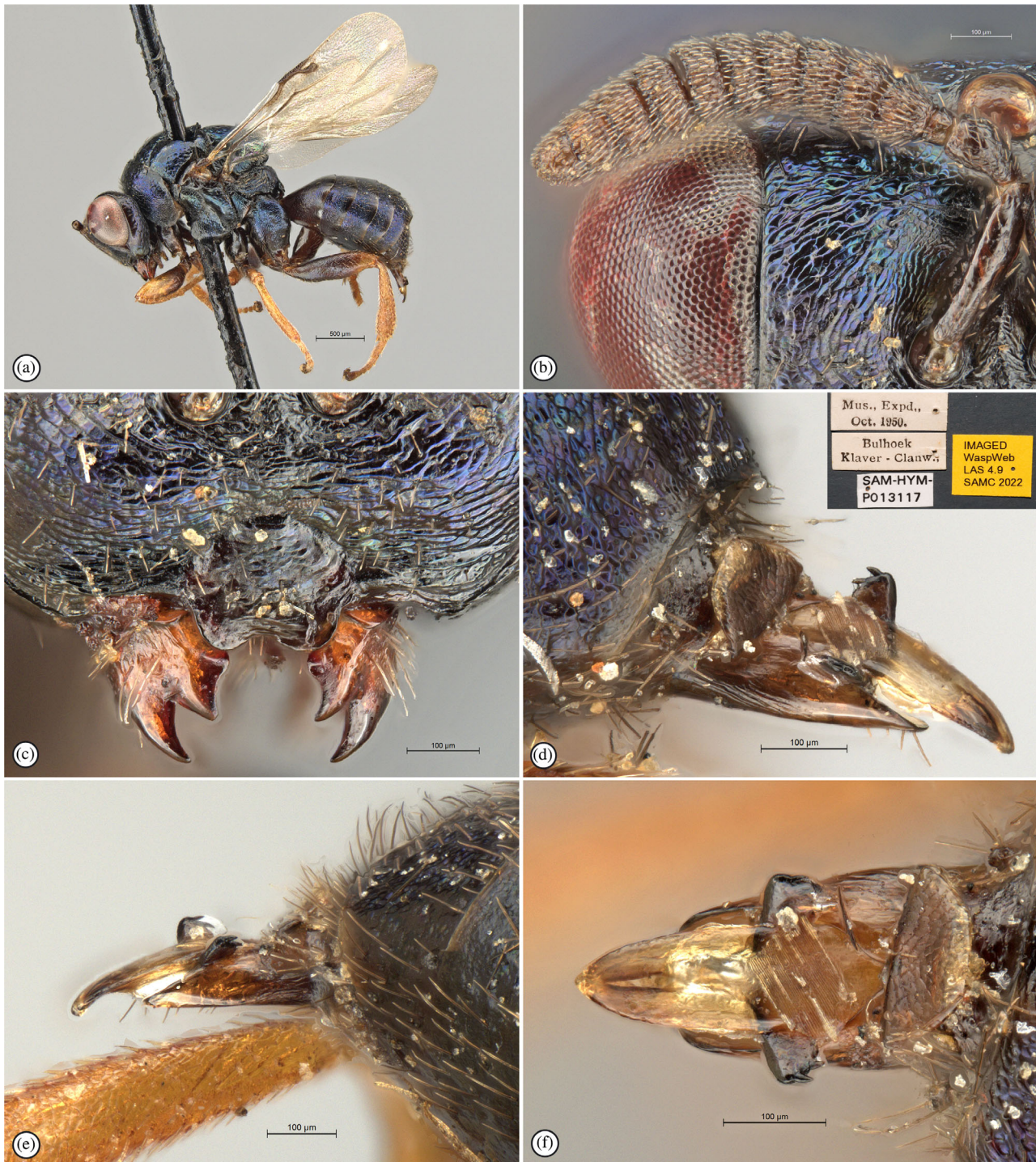
FIGURE 21 *Asparagobius bouceki* van Noort, sp. nov., paratype ♂ SAM-HYM-P013117 (SAMC). (a) habitus, lateral view; (b) antenna, lateral view; (c) clypeus, mandibles, anterior view; (d) genitalia, dorso–lateral view (inset: data labels); (e) genitalia, lateral view; (f) genitalia, dorsal view.

differentiated by notaular depressions, these strongly impressed posteriorly, irregularly foveate and weak and shallow in anterior half (Figure 19e). Mesoscutellum as long as wide; axillular grooves not sulcate, evident as strong depressions. Axillae concave, laterally bounding the central strongly raised mesoscutellum structured as an evenly rounded hump (Figure 19d). Mesopleuron and metapleuron bare, except for a few strong white setae dorsally on mesopleuron. Mesepimeron densely covered with strong white setae (Figure 18d). Propodeum anteriorly with transverse row of weak fovea extending posteriorly as narrow, reticulate, medial band to defined nucha; lateral areas roughly sculptured; dense patch of strong white setae around spiracles (Figure 19d). Metacoxa large, without white setae dorsally and ventrally; metafemur 4.5× as long as broad; metatibia straight, 4.6× as long as broad

FIGURE 22 *Asparagobius braunsi* ♀ (SAM-HYM-P021373a). (a) habitus, lateral view (inset: data labels); (b) habitus, dorsal view; (c) head, mesosoma dorsal view; (d) head, mesosoma, lateral view; (e) gaster, lateral view; (f) wings.

(Figure 18a). Fore wing with postmarginal vein equal in length to stigmal vein and $0.75\times$ marginal vein length; submarginal vein with 10–12 weak sensilla and thickened in apical third; stigmal vein cleaver-shaped (Figure 18e). Hind wing with 3 long hamuli, venation strong, angular (Figure 18e).

Gaster. Gaster circular in dorsal view, as long as wide, $0.93\times$ mesosoma length; Gt_1 longest, equivalent in length to Gt_2 and Gt_3 combined; Gt_2 extremely short dorsally, largely hidden beneath Gt_1 (Figure 19f). Hypopygium short, recessed with medial invagination (Figure 20d). Ovipositor sheaths short, contained within medial, longitudinally concave excavation within Gt_8, not reaching cerci, apically with tuft of setae (Figure 20d). Male genitalia depicted in Figure 21d–f.
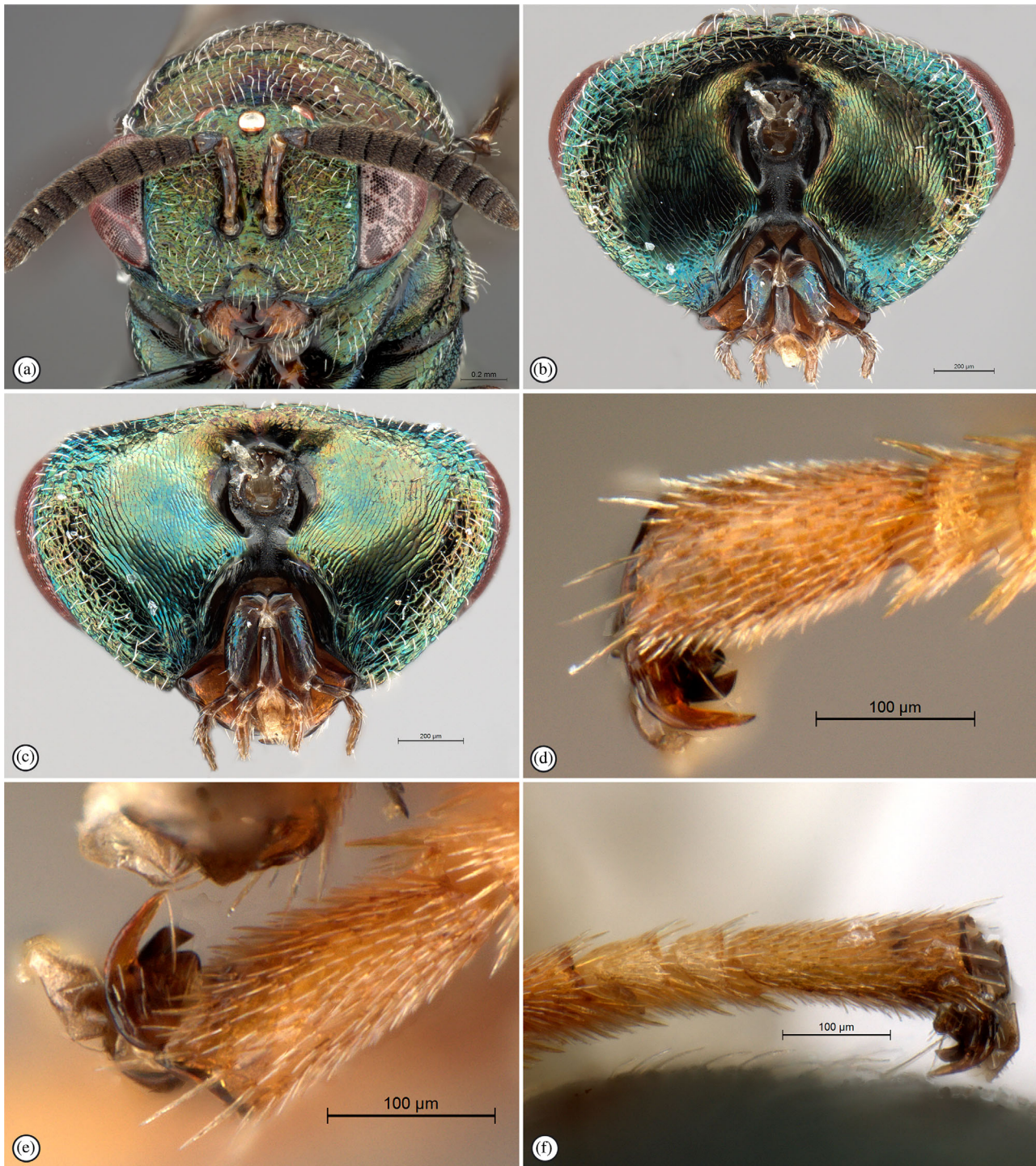
FIGURE 23 *Asparagobius braunsi* ♀ (a–e) (SAM-HYM-P021373b) and ♂ (F) (SAM-HYM-P021373c). (a) head, anterior view; (b) head, posterior view; (c) head, posterior–ventral view; (d) female metatarsal claw, adaxial view; (e) female metatarsal claw, axial view; (f) male metatarsal claw, axial view.

Asparagobius braunsi Mayr, 1905 (Figures 22–27).

Asparagobius braunsi Mayr, 1905. Holotype: ♀ in the Natural History Museum, Vienna. Type locality: Willowmore, South Africa.

Additional material examined. 45♀ 5♂ SOUTH AFRICA: *Eastern Cape, Cape Col, Kentani, Peglar,? Asparagobius* det. E. Grissell, 1996, SAM-HYM-P009894, SAM-HYM-P002931 (SAMC); 12♀ 1♂ Blauwe Krans

Farm, (12.8 km 216° SW Kirkwood) 33°30.747′S 25°24.644′ E, Emerged 23–27 Feb 2001, S. van Noort, ex gall on *Asparagus striatus*, Valley Bushveld, *Asparagobius braunsi* Mayr, det. S. van Noort 2001, IMAGED WaspWeb, LAS 4.9, SAMC 2018 and 2022, SAM-HYM-P021373 (SAMC).

Diagnosis. Metapleuron rhomboidal, with truncate dorsal margin (Figure 22d); fore wing with extensive dark infuscation below venation (Figure 22f); marginal vein twice length of postmarginal and
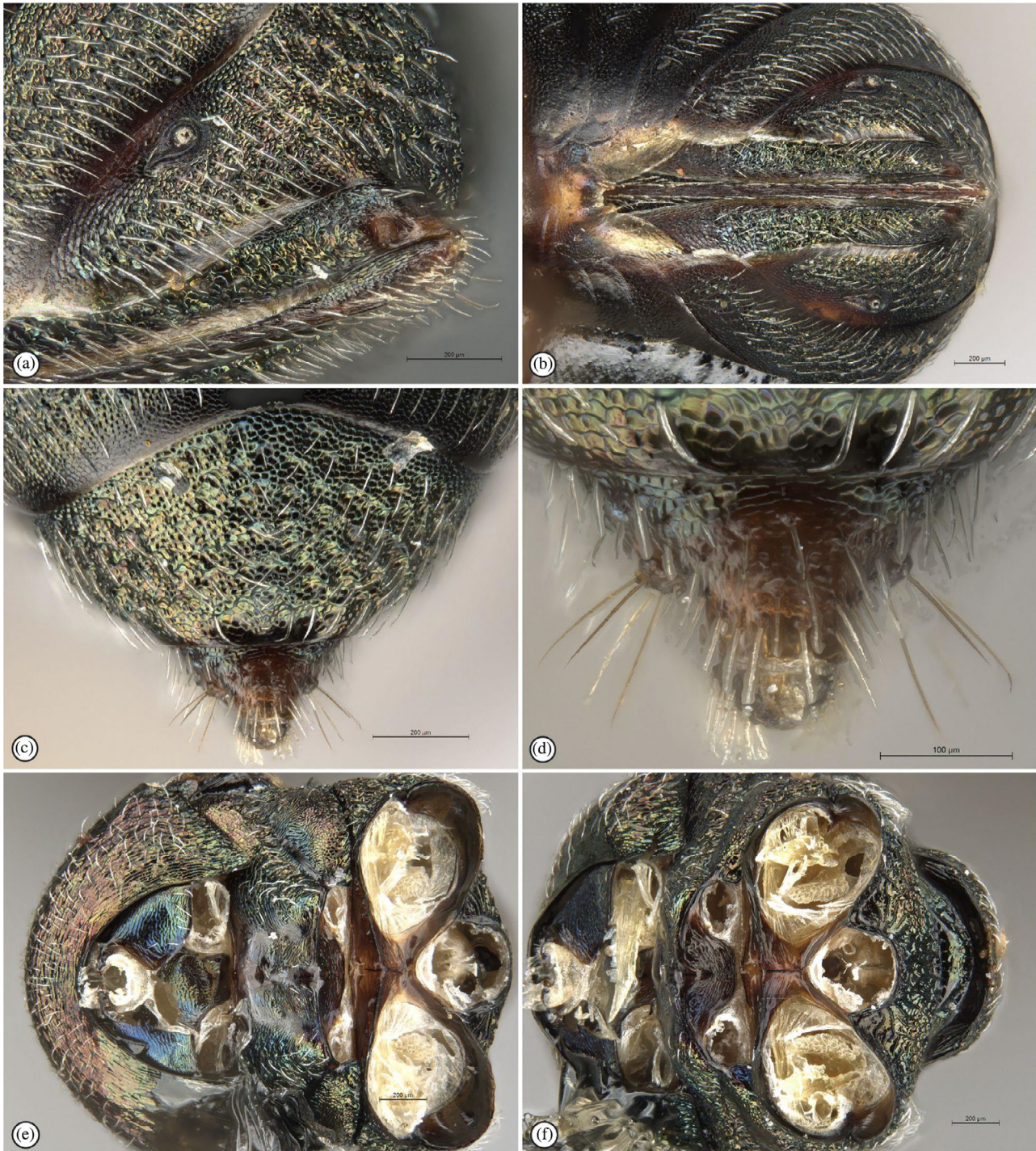
REDEFINING ORMYRIDAE

Systematic
Entomology

Royal
Entomological
Society

21

FIGURE 24 *Asparagobius braunsi* ♀ (SAM-HYM-P021373d). (a, b) gastral terminal tergites, ovipositor: (a) ventrolateral view; (b) ventral view; (c) dorsal view. (d) gastral tergite 8, dorsal view; (e) mesosoma, ventral view; (f) mesosoma, posterior view (dorsum to right).

stigmal vein (Figure 22f); gaster sparsely setose except for dorsal bare area (Figure 22b); body metallic green–bronze (Figure 22a).

Differential diagnosis. The metapleuron is triangular, the fore wing hyaline and the body metallic blue in *A. bouceki*, whereas *A. copelandi* differs by having the marginal, postmarginal and stigmal veins equivalent in length and the gaster more densely setose with the body matt black.

Biology. Phytophagous gall former on *Asparagus striatus* and *Asparagus divaricatus* (Asparagaceae) (Figures 25–27).

Distribution. South Africa.

***Asparagobius copelandi* Rasplus and van Noort, sp. n.** (Figures 28 and 29).

FIGURE 25 *Asparagobius braunsi* galls and adult. (a) gall on *Asparagus striatus*; (b) gall split open; (c) developing *A. braunsi* larvae and pupae in situ in gall locules; (d) adult *A. braunsi* chewing her way out of gall; (e) recently emerged adult *A. braunsi*, laterodorsal view; (f) recently emerged adult *A. braunsi*, dorsal view. Photographs by Sally Adam (https://www.inaturalist.org/observations/54615403).

LSID urn:lsid:zoobank.org:act:C90B9FB8-12B4-4DE8-9B36-1AC0AD ABD86E.

Holotype: KENYA, *Coast Province*, Diani Beach area, alt. 10 m, −4.27559° N, 39.59337° E, 2014, coll. Copeland R. Deposited in ICIPE.

Paratype. 1 F: same data as holotype (CBGP).

Diagnosis. Metapleuron rhomboidal, with truncate dorsal margin (Figure 28g); fore wing with small dark infuscate region below venation (Figure 28b); marginal, postmarginal and stigmal veins equivalent

REDEFINING ORMYRIDAE

Systematic
Entomology

Royal
Entomological
Society

23

FIGURE 26 *Asparagobius braunsi* galls on *Asparagus striatus*. (a) young galls in situ. Photograph by Tony Rebelo (https://www.inaturalist.org/observations/13388631); (b) young and old galls in situ. Photograph by Wendy Wiles (https://www.inaturalist.org/observations/11204361); (c) old galls in situ. Photograph by Sandra Falanga (https://www.inaturalist.org/observations/50974847); (d) old gall in situ. Photograph by Sally Adam (https://www.inaturalist.org/observations/30950934).

in length (Figure 28c); gaster densely setose except for dorsal bare area (Figures 28b and 29b); body matt black (Figure 28); propodeum strongly rugulose (Figure 28e).

Differential diagnosis. *Asparagobius bouceki* is metallic blue, the metapleuron is triangular and the fore wing is hyaline, whereas *A. braunsi* is metallic green–bronze, the marginal vein is twice the length of the postmarginal and stigmal veins, and the gaster is less setose.

Etymology. Named in recognition of the efforts of Robert Copeland (ICIPE) in conducting inventory surveys of the Hymenoptera fauna of East Africa using Malaise traps. Noun in genitive case.

Biology. Unknown, specimens collected in Malaise traps.

Distribution. Kenya.

Description. Body length 3.4 mm.

Colour. Body almost entirely matt black, with some dark red–brown areas on mesosoma antero–ventrally and on metafemur, and yellow–brown on rest of legs and scape and pedicel; fore wing with small area of infuscation; venation light brown; eyes and ocelli red–brown; setae white (Figure 28a–g).

Head. Scape $4.45\times$ as long as broad, extending four-fifths of distance to median ocellus; pedicel short, as long as wide, and globular, as long as fl_2, and with scattered long setae; flagellum as long as head height, with a short, transverse anellus, seven funiculars and three clavomeres; flagellum broadened at anellus and funiculars approximately of same width; flagellum tapering gradually through clava; club undifferentiated in structure from funiculars; fl_2 $1.25\times$ longer than broad, remaining funiculars transverse, $3\times$ broader than long; all funiculars and clavomeres with many tiny, densely packed multiporous plate sensilla interspersed in many rows (Figure 28a). Mandibles equally stout, each with two strong, acute teeth apically (inner tooth shorter than apical tooth) and a short, blunt, third molar tooth basally. Head sculpture imbricate, and with strong, white, scattered setae (Figure 28d). Interantennal process weak. Toruli separated from each other by two thirds of torulus diameter (Figure 28d). Eyes with small, scattered white setae; interocular distance $1.9\times$ eye

FIGURE 27 *Asparagobius braunsi* galls on *Asparagus divaricatus*. (a) old gall in situ. Photograph by Graham Grieve (https://www.inaturalist.org/observations/70816950); (b) young and old galls in situ. Photograph by Graham Grieve (https://www.inaturalist.org/observations/70816950); (c) and (d) recently emerged adult *A. braunsi* from *A. divaricatus* gall. Photographs by Graham Grieve (https://www.inaturalist.org/observations/10959290).

height; inner eye margins subparallel to each other, slightly converging ventrally; malar space 0.5× eye height. Ocellar triangle raised. POL:OOL:LOL = 12:6:5. Antennal scrobe shallow and broad, with rounded margins, narrowly and shallowly extending to median ocellus. Anterior tentorial pits evident as slight depressions (Figure 29a). Clypeus as wide as high, slightly convex overall; clypeal margin strongly projected, bilobed with shallow, obtuse, medial triangular indentation (Figure 28d). Labrum hidden. Occipital carina present dorsally, gently curved, but medially humped; postgenal lamina absent; subforaminal bridge with postgenae narrowly separated, lower tentorial bridge slightly sunken; posterior tentorial pits situated lateral of upper foramen magnum; secondary posterior tentorial pits deep and long, positioned lateral to lower foramen magnum and dorsal half of tentorial bridge; hypostomal carinae hardly evident, not extending to posterior tentorial pits, fading two-thirds up oral fossa (Figure 29a). Pom present along a broad median area encompassing width of lower tentorial bridge (Figure 29a).

Mesosoma. Pronotum, mesoscutum and mesoscutellum with scattered strong white setae (Figure 28f,g). Mesoscutum 1.85× as broad as long, 1.1× length of mesoscutellum; mesoscutal lobes differentiated by weak and shallow notaular depressions, indicated only by difference in sculpture (Figure 28f). Mesoscutellum 1.25× wider than long; axillular grooves not sulcate, evident as strong depressions demarcated by a line of fovea. Axillae concave, laterally bounding the central strongly raised mesoscutellum structured as a hump with posterior three-quarters flat in profile (Figure 28f). Mesopleuron and metapleuron medially bare, but mesopleuron with patch of strong white setae anteriorly and posteriorly, and metapleuron with antero–ventral patch of strong white setae. Mesepimeron densely covered with strong white setae (Figure 28g). Propodeum strongly rugulose; nucha short, weakly defined; dense patch of strong white setae lateral of spiracles (Figure 28e). Metacoxa large, with patches of strong white setae dorsally and ventrally; metafemur 4.3× as long as broad; metatibia straight, 4.5× as long as broad (Figure 28b). Fore wing with postmarginal 0.75× length of stigmal vein and 0.5× marginal vein length; submarginal vein with 8 weak sensilla, and not thickened in apical third; stigmal vein club-shaped (Figure 28b). Hind wing with 3 long hamuli, venation weak, faint, angular.

REDEFINING ORMYRIDAE

Systematic
Entomology

Royal
Entomological
Society

25

FIGURE 28 *Asparagobius copelandi* Rasplus and van Noort, sp. nov., holotype ♀ (ICIPE). (a) antenna, axial view; (b) habitus, lateral view; (c) fore wing venation; (d) head, anterior view; (e) metanotum, propodeum, dorsal view; (f) head, mesosoma, dorsal view; (g) head, mesosoma, lateral view. Scale bar = 0.5 mm, except for B = 1 mm.

FIGURE 29 *Asparagobius copelandi* Rasplus and van Noort, sp. nov., holotype ♀ (ICIPE). (a) head, ventral view; (b) gaster, dorsal view; (c) gaster, ventral view; (d) gastral terminal tergites, ovipositor, ventral view.

Gaster. Gaster $1.4\times$ longer than wide, $1.3\times$ mesosoma length; Gt_1 longest, $2\times$ length of each of Gt_2, Gt_3, Gt_4 and Gt_5 (Figure 29b). Hypopygium short, recessed with medial invagination (Figure 29c). Ovipositor sheaths short, contained within medial, longitudinally concave excavation within tergite 8, not reaching cerci, without a tuft of setae (Figure 29d).

Halleriaphagus van Noort and Burks, gen. nov. (Figures 30–35). LSID urn:lsid:zoobank.org:act:99FBB231-F961-4F13-8319-FAB111C2C82B.

Type species: *Halleriaphagus phagolucida* van Noort and Burks, **sp. nov.**

Diagnosis. Clypeus narrow, as high as wide (Figure 31c); clypeal margin strongly projected, bilobed with strong setae (Figure 31c); clypeus encompassed by a broad, triangular, concave area, the medial height of which is a third its width, with dorsal triangular apex extending as medial linear area of smaller sculpture to depression surrounding antennal toruli (Figure 31c). Antennal formula 11264; multiporous plate sensilla large, in one to two rows on each flagellomere (Figure 31d); occipital carina present dorsally, gently curved (Figure 2b); postgenal lamina present (Figure 2b); tarsal claw with large basal projection that is cleft (Figure 33b, c); stigmal vein at c. an 80 degree angle to postmarginal vein, club-shaped, subequal in length to postmarginal vein and half as long as marginal vein (Figures 31f and 33d), and with uncus small, hardly protruding in female (Figure 31f) but strongly protruding in male (Figure 33d).

Etymology. Named in recognition of gall formation on *Halleria lucida* and *H. elliptica*. A combination of the host plant genus name *Halleria* with the Latin word *phagus* meaning to eat, derived from Ancient Greek -φάγος (-phágos, '-eating'), latinized to *phagus*. Hence the gender is masculine.

Biology. Reared from leaf galls on *Halleria lucida* and *H. elliptica* (Stilbaceae) (Figures 34 and 35).

Distribution. South Africa.

Description.

Head. Antenna with 12 flagellomeres; flagellum with two anelli, the first subquadrate and second wider than long,

REDEFINING ORMYRIDAE

Systematic
Entomology

Royal
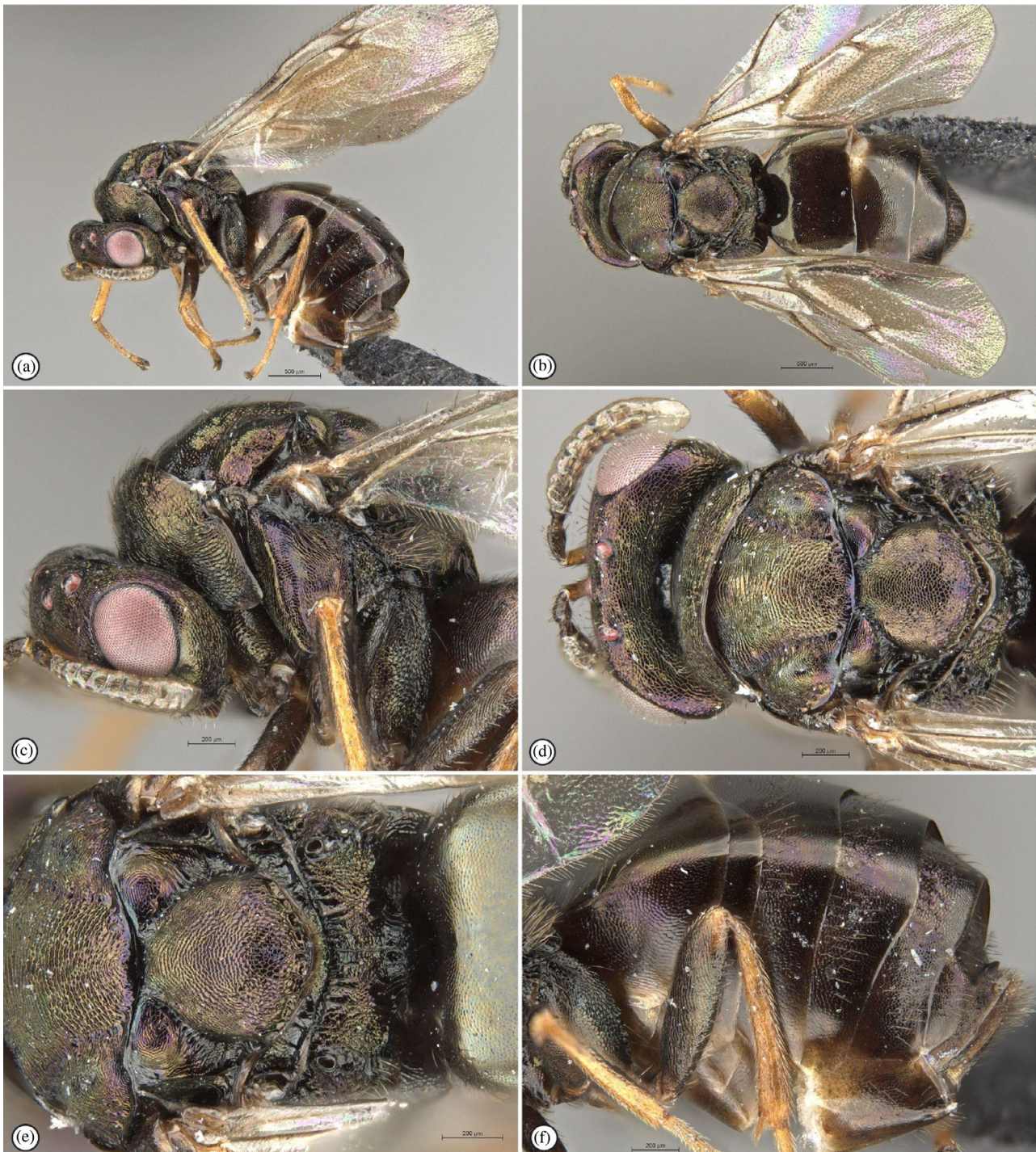Entomological
Society

27

FIGURE 30 *Halleriaphagus phagolucida* van Noort and Burks, sp. nov., holotype ♀ (SAM-HYM-P086327). (a) habitus, lateral view; (b) habitus, dorsal view; (c) head, mesosoma, lateral view; (d) head, mesosoma, dorsal view; (e) mesoscutum, propodeum, dorsal view; (f) gaster, lateral view.

clava undifferentiated in structure from funiculars (Figure 31d). Mandibles each with two strong, prominent, teeth subequal in size and length, and a third small basal tooth (Figure 31c). Maxillary palp 4-segmented, distal segment longest, subequal in length to basal three segments combined, labial palp 3-segmented, distal segment longest and widest, subequal in length to basal two segments combined (Figure 31b). Antennal scrobe shallow and broad, with rounded margins, not extending to median ocellus. Anterior tentorial pits not easily visible, evident as depressions. Clypeus narrow, as high as wide, convex dorsally between tentorial pits, depressed medially and anteriorly; clypeal margin strongly projected, bilobed with strong setae; clypeus encompassed by a broad, triangular, concave area, medial height of which is a third its width, with dorsal triangular apex extending as medial linear area of smaller

FIGURE 31 *Halleriaphagus phagolucida* van Noort and Burks, sp. nov., (a,b) paratype ♀ (SAM-HYM-P086328); (c–f) holotype ♀ (SAM-HYM-P086327). (a) head, posterior view; (b) head, posterior–ventral view; (c) head, anterior view; (d) antenna, anti-axial view; (e) gastral terminal tergites, ovipositor, ventral view; (f) fore wing.

sculpture to depression surrounding antennal toruli (Figure 31c). Labrum hidden. Malar sulcus present as a broad depression, complete. Gena sculpturally undifferentiated posteriorly. Occipital carina present dorsally, gently curved; postgenal lamina present, encompassing foramen magnum dorsally, extending laterally for short distance; subforaminal bridge with postgenae separated, lower tentorial bridge sunken; secondary posterior tentorial pits deep and long, positioned lateral to lower foramen magnum and dorsal half of tentorial bridge; hypostomal carinae not extending to posterior tentorial pits, fading when reaching lower tentorial bridge, with polished, narrow differentiated hypostomal area (Figures 2b and 31a). Pom present along a broad median area (Figure 2b).
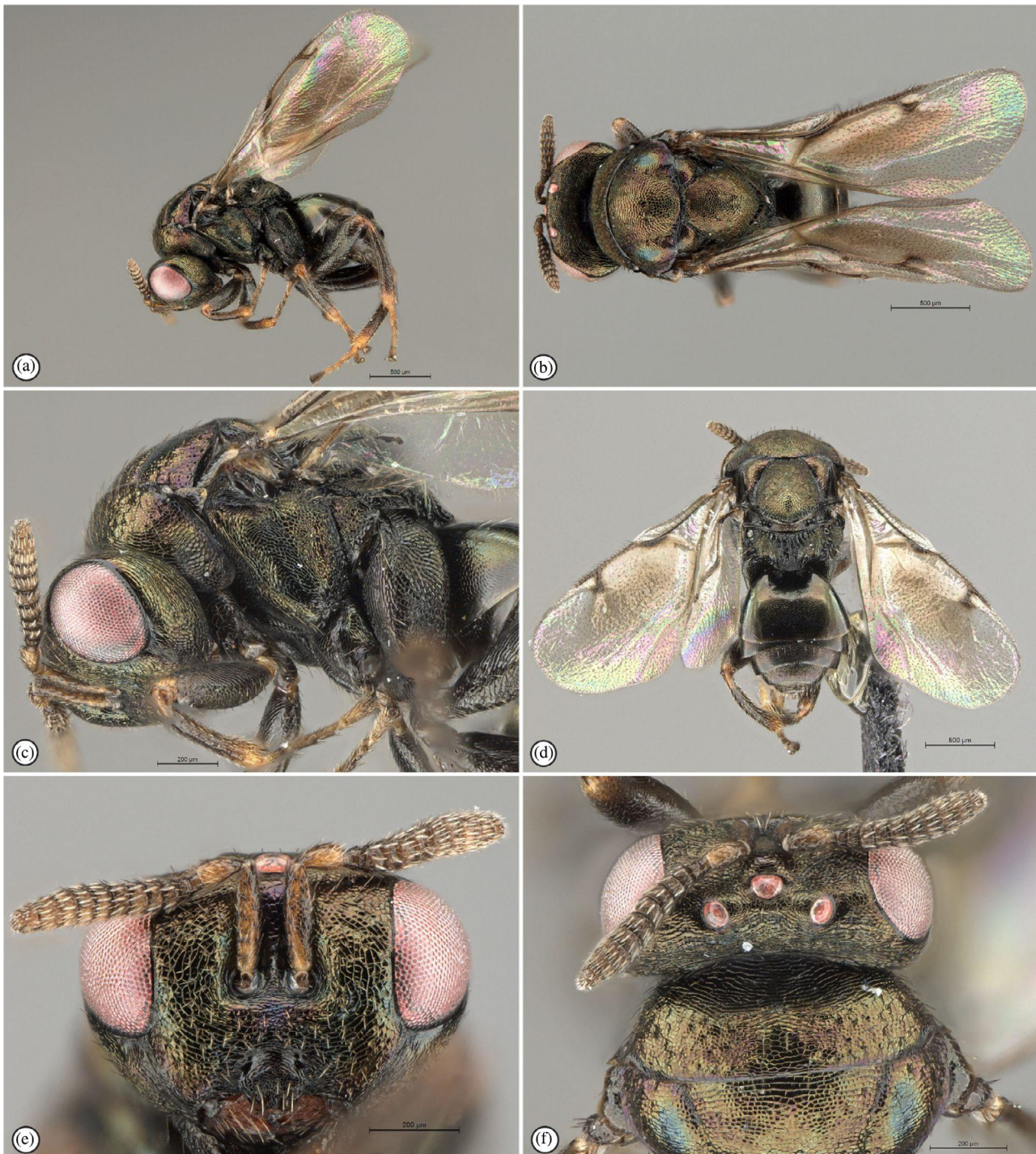
FIGURE 32 *Halleriaphagus phagolucida* van Noort and Burks, sp. nov., paratype ♂ (SAM-HYM-P088414). (a) habitus, lateral view; (b) habitus, dorsal view; (c) head, mesosoma, lateral view; (d) body, dorsal view; (e) head, anterior view; (f) head, pronotum, dorsal view.

Mesosoma. Pronotum short, about 4× wider than long, with short, broad neck (Figure 32f). Mesoscutum with weakly foveate, complete, depressed notauli. Scutoscutellar suture simple, axillular sulcus strongly depressed, weakly foveate. Frenal arms strong; mesoscutellar rim foveate (Figure 30e). Prepectus laminar, slightly overlapping mesoscutum, mesopleuron and tegula, bluntly rhomboidal

(Figure 3b). Fore wing with scattered, dark, microtrichia and short marginal fringe (Figure 31f); basal and cubital folds pigmented, stigmal vein at c. an 80 degree angle to postmarginal vein, club-shaped, subequal in length to postmarginal vein and half as long as marginal vein (Figure 31f), and with uncus small, hardly protruding in female (Figure 31f) but strongly protruding in male (Figure 33d); wing disc

FIGURE 33 *Halleriaphagus phagolucida* van Noort and Burks, sp. nov., paratype ♂ (SAM-HYM-P088414). (a) mesosoma, gaster, dorsal view; (b) protarsal claws; (c) protarsal claws; (d) fore wing (inset: data labels).

pigmented over a broad area below venation. Legs with five tarsomeres; tarsal claws with large basal projection that is cleft (Figure 33b,c).

Gaster. Gaster non-collapsing, but with separate tergites (Figures 30f and 33a); Gt$_1$ without dorsal longitudinal carinae; syntergum in female with depression, separated by a median carina, surrounding cercus.

***Halleriaphagus phagolucida* van Noort and Burks, sp. nov.**
(Figures 30–35).
LSID urn:lsid:zoobank.org:act:7076B135-C1BA-400F-8CE3-160EC420E05D.

Holotype. ♀. SOUTH AFRICA: *Western Cape*, Tsitsikamma National Park, Diepwalle forest, −33.960885° 23.161130°, 471 m, gall collected 8 July 2021, emerged 21 July 2021, RC Swart, Afromontane Forest, ex *Halleria lucida* leaf galls, SAM-HYM-P086327. Deposited in SAMC.

Paratypes. SOUTH AFRICA. 2♀ 1♂: *ditto*, SAM-HYM-P086326, SAM-HYM-P086328, SAM-HYM-P086329. 8♀ 3♂, 1 larva (mounted): *Western Cape*, Tsitsikamma National Park, Diepwalle forest,

−33.960885° 23.161130°, 471 m, 8 July 2021, emerged 21 July 2021, RC Swart, Afromontane Forest, ex *Halleria lucida* leaf galls, SAM-HYM-P095137 to SAM-HYM-P095141, SAM-HYM-P095143, SAM-HYM-P095145 to SAM-HYM-P095148, SAM-HYM-P095150, SAM-HYM-P095151 (SAMC); 1♀, 1♂: *Kwazulu-Natal*, St Lucia, 28.3728S 32.3912E, 20–30 Dec 2019, MJ Botha, ex gall on *Halleria lucida* (iNat observation 37,128,221), coastal forest, Ormocerinae det. S. van Noort 2019, SAM-HYM-P088414, SAM-HYM-P088415 (SAMC); 1♀ 1♂ (plus dried hard woody host gall) *Kwazulu-Natal*, Munster, 40 m, 30° 59.965′ S 30° 15.599′ E, G. Grieve, 9 June 2014, emerged October 2014, ex stem galls on *Halleria lucida* SAM-HYM-P048077 (SAMC); 6♀, 1♂: *Eastern Cape*, Kentani, Miss A. Peglar, bred from galls on *Halleria elliptica*, 1♀ remounted on point from original communal card, IMAGED WaspWeb LAS 4.9 SAMC 2022, SAM-HYM-P009897A (SAMC); 1♂ remounted on point from original communal card SAM-HYM-P009897B (SAMC); 5 remaining ♀ remain mounted on original communal card SAM-HYM-P009897C to SAM-HYM-P009897F (SAMC); 1♀: Grahamstown, S. Africa, Nov. 1951, E. Mc C. Callan, ex stem gall on *Halleria lucida* L. (NHMUK).

Diagnosis. As for genus.

REDEFINING ORMYRIDAE

Systematic
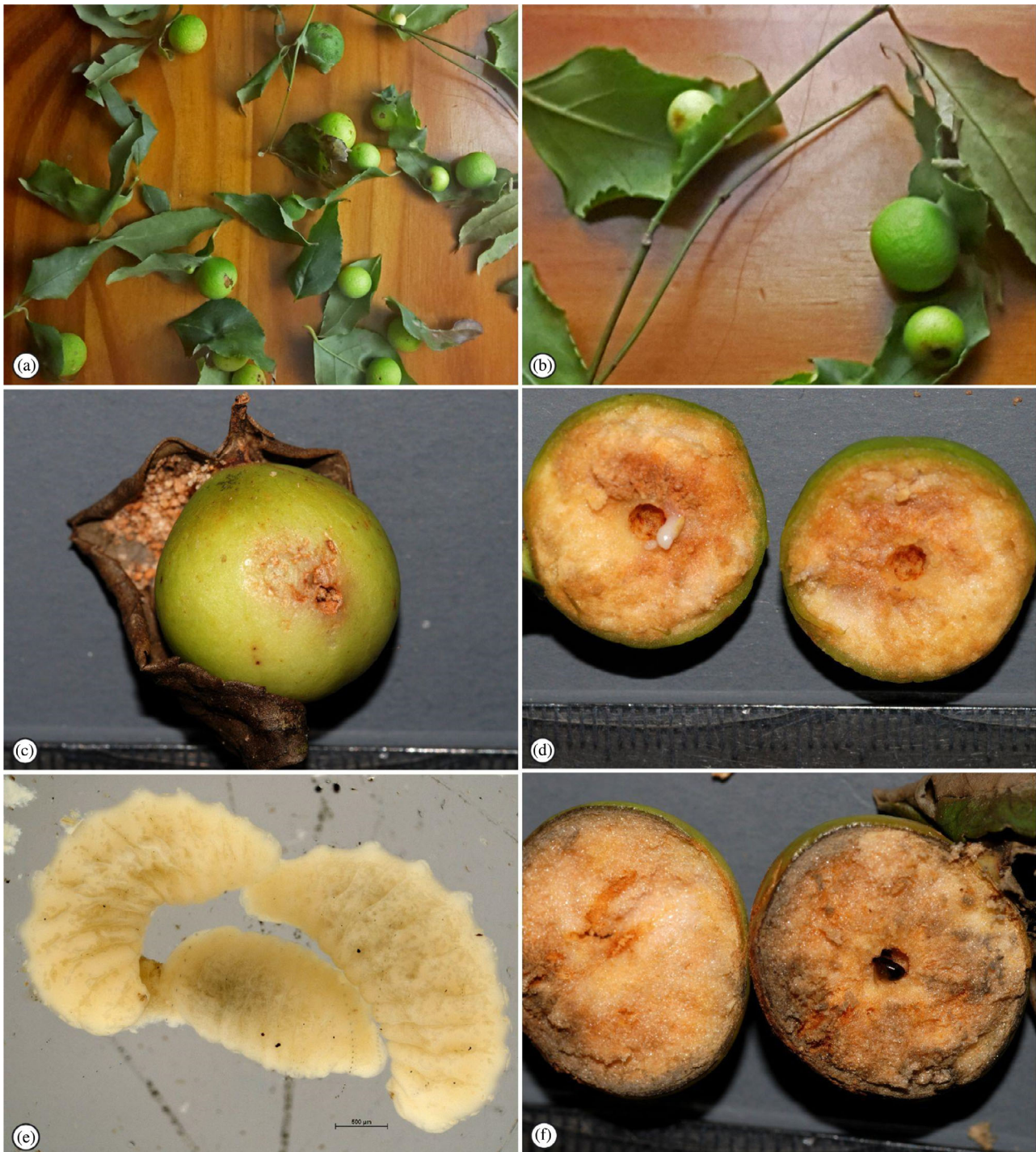Entomology

Royal
Entomological
Society

31

FIGURE 34 *Halleriaphagus phagolucida* van Noort and Burks, sp. nov., host galls on host plant *Halleria lucida* (SAM-HYM-P086326 to P086329) from Diepwalle. (a, b) galls in situ on leaves; (c) gall with *H. phagolucida* exit hole; (d) split open gall showing central locule with developing *H. phagolucida* larva; (e) three developing *H. phagolucida* larvae each extracted from a central locule in three different galls; (f) split open gall showing central locule with mature *H. phagolucida* adult.

Etymology. Named in recognition of gall formation on *Halleria lucida*. A combination of the host plant species epithet *lucida* with the Latin word *phagus* meaning to eat. Noun in apposition.

Biology. Reared from leaf galls formed on *Halleria lucida* and *Halleria elliptica* (Stilbaceae) (Figures 34 and 35).

Distribution. South Africa.

Description. Body length 2.5–3.5 mm.

Colour. Body almost entirely metallic green–bronze, with some purple lustre, becoming yellow–brown on areas of the
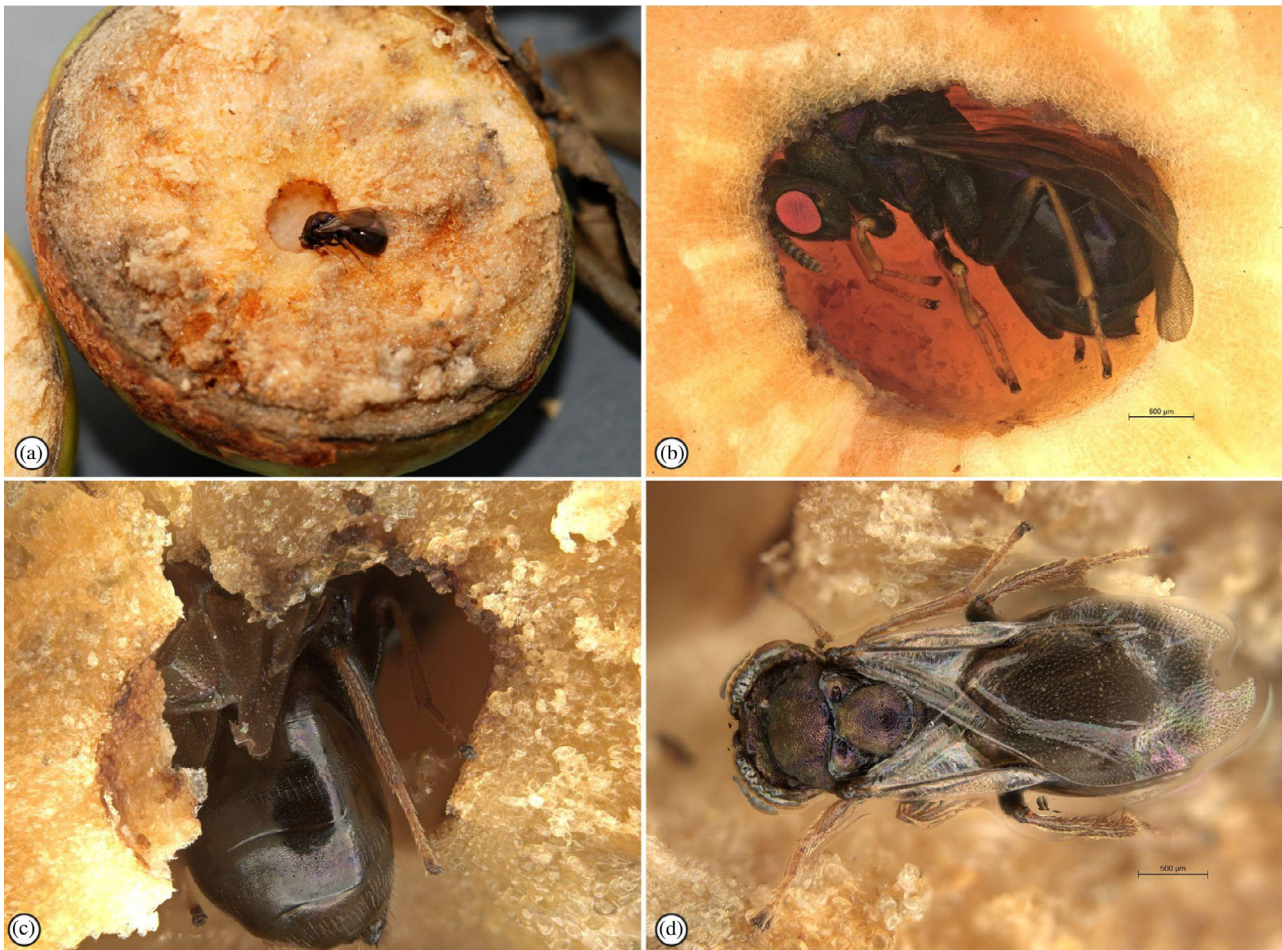
FIGURE 35 *Halleriaphagus phagolucida* van Noort and Burks, sp. nov., host galls on host plant *Halleria lucida* (SAM-HYM-P086326 to P086329) from Diepwalle. (a–c) split open gall showing central locule with mature *H. phagolucida* adult; (d) recently emerged *H. phagolucida* adult.

legs and flagellum; venation dark brown; eyes and ocelli pink–white; setae white (Figure 30a–f).

Head. Scape 5× as long as broad almost extending to median ocellus; pedicel as long as $fl_1 + fl_2 + fl_3$, with scattered long setae; flagellum length equal to head height, with a subquadrate first anellus, transverse second anellus, six funiculars and four clavomeres; funicle broadening distally; fl_3 1.5× broader than long, as long as fl_3, and with only a few multiporous plate sensilla; all other funiculars and clavomeres transverse, with one dominant row of multiporous plate sensilla, but distal five funiculars occasionally interspersed with second sparse row of sensilla (Figure 31d). Head sculpture imbricate, and with scattered setae (Figure 31c). Interantennal process present but weak. Toruli separated from each other by less than diameter of a torulus. Eyes with small, scattered setae; interocular distance 1.5× eye height; inner eye margins subparallel; malar space 0.6× eye height (Figure 31c). Clypeus with about 8–10 strong setae (Figures 31c and 32e). Ocellar triangle raised. POL:OOL: LOL = 14:7:6 (Figure 32f). Vertex posterior of ocellar triangle and occiput transversely strigose (Figure 30d).

Mesosoma. Pronotum, mesoscutum and mesoscutellum with scattered long setae (Figure 30d). Mesoscutum twice as broad as long, 0.9× length of mesoscutellum; mesoscutal lobes differentiated by notaular depressions (Figure 30d). Mesoscutellum length 1.1× width; axillular grooves distinct, depressed, weakly foveate and distinctly and evenly broadening posteriorly (Figure 30e). Mesopleuron and metapleuron bare, except for a few setae dorsally and ventrally (Figure 30c). Propodeum anteriorly with weak, short longitudinal carinae flanking polished areas, these polished areas also present around spiracles, but remaining surface reticulate with a single median carina extending to nucha in female (Figure 30e) and five broken carinae extending to nucha in male (Figure 30a). Metacoxa large, metafemur, 4× as long as broad; metatibia gently curved, 7× as long as broad (Figure 30a). Fore wing with postmarginal vein 1.4× (female) and 1.25× (male) length of stigmal vein, and 0.5× marginal vein length; submarginal vein with 10–12 strong sensilla; stigmal vein club-shaped (more strongly clavate in male due to strongly projecting uncus; uncus small, hardly projecting

FIGURE 36 *Hemadas nubilipennis* ♀ (CNC). (a) habitus, lateral view; (b) head, mesosoma, dorsal view; (c) head, anterior view; (d) toruli, face and clypeus, anterior view; (e) antenna dorso–lateral view.

in female) (Figures 31f and 33d). Hind wing with 3 long hamuli, venation strong, angular (Figure 33d).

Gaster. Gaster globular, length 1.25× width, 1.4× mesosoma length; Gt_1 longest, twice length of Gt_3 and Gt_4 in female and half of total gaster length in male; Gt_2 extremely short, largely hidden beneath Gt_1 (Figures 30f and 33a). Hypopygium short, blunt (Figure 17e). Ovipositor sheaths short, held

dorsally in close apposition to Gt_8, hardly extending beyond position of cerci, and ventrally with dense tuft of long setae (Figure 31e).

Variation. The older Kentani specimens in SAMC that were reared at the turn of last century from *H. elliptica* have the clypeal margin more deeply bilobed with the clypeus

FIGURE 37 *Hemadas nubilipennis* ♀ (CNC). (a) head, mesosoma, lateral view; (b) mesosoma, lateral view (wings removed); (c) prepectus, mesopleuron, lateral view; (d) propodeum, dorsal view; (e) fore wing venation; (f) wings.

projecting, narrower than high. The pedicel is shorter than in the holotype, only as long as the anellus and first funicular combined; the anellus is narrower, much shorter than the first funicular (the anellus is quadrate, as long as first funicular in the holotype); occipital carina gently curved with a strong and narrow dorso–medial indentation (indentation absent in holotype); anterior mesoscutellar margin broad, longer than anterior axillar margin (narrow in holotype); body with metallic purple iridescence, which is probably an artefact of age and exposure to pesticides used in the insect drawers. The freshly reared specimens have a metallic greenish–purple iridescence.

FIGURE 38 *Hemadas nubilipennis* ♀ (UCR). (a) head, anterior view; (b) head, posterior view; (c) mesosoma, lateral view; (d) mesosoma dorso–lateral view; (e) terminal gastral tergites; postero–ventral view; (f) fore tarsus distal view, showing tarsal claw, ventral view.

Hemadinae van Noort, Burks, Mitroiu and Rasplus, subfam. nov.

LSID   urn:lsid:zoobank.org:act:A30D16F2-D67A-4CD5-B747-488E412775B1.

Type genus: *Hemadas* Crawford, 1909.

Diagnosis. Antennal formula 11264 (Figure 36e); multiporous plate sensilla large, in one or two irregular rows on each funicular (Figure 36e); clypeus with apical margin almost straight, but wavey, at most broadly and shallowly emarginate medially (Figure 36d); postgenal bridge open, separated by lower tentorial bridge (Figures 2d and 38b); postgenal lamina absent (Figures 2d and 38b); frenal line carinate laterally, but medially indicated only by more or less a change in sculpture; stigmal vein at c. an 80° angle to postmarginal vein, club-shaped, uncus very long (Figure 37e); tarsal claws with rudimentary hump (Figure 38f).
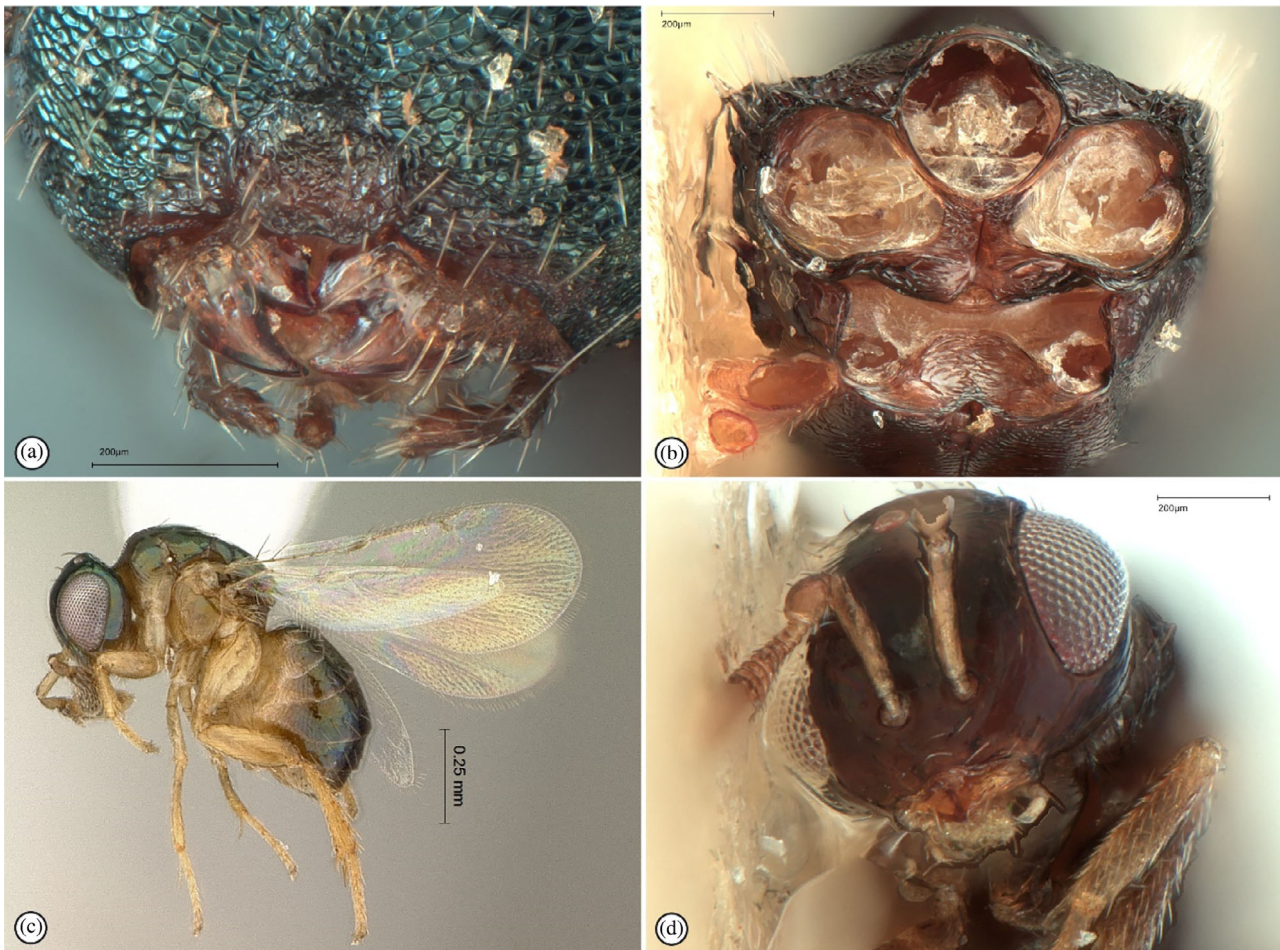
FIGURE 39 (a, b) *hemadas nubilipennis* ♀ (CNC); (c, d) *Ormyrus gibbus* (UCR). (a) clypeus and mandibles, anterior view; (b) mesosoma, posterior view (legs removed, dorsal surface towards top); (c) habitus, lateral view; (d) head anterior view.

Distribution. Nearctic region.

Hemadas Crawford, 1909 (Figures 36–39).

Hemadas Crawford, 1909. **Type species**: *Megorismus nubilipennis* Ashmead, 1887.
Parhabritys Girault, 1917. Synonymy by Gahan and Ferrière (1947).

Diagnosis. The same as for subfamily.

Biology. *Hemadas nubilipennis* (Ashmead) is a gall former on Blueberry, *Vaccinium angustifolium* (Ericaceae) (MacKay, 1989; McAlister & Anderson, 1932; Shorthouse et al., 1986, 1990; West & Shorthouse, 1989). *Hemadas* is commonly known as the Blueberry stem gall wasp. Attacked by at least three parasitoid wasps: *Ormyrus vacciniicola*, *Eurytoma solenozophaeriae* and *Sycophila vacciniicola* (latter both Eurytomidae) (Isaacs et al., 2020).

Distribution. Nearctic (Canada, USA).

Species richness. *Hemadas nubilipennis* (Ashmead, 1887).

Ormyrinae Förster, 1856

Diagnosis Antennal formula 11354, 11264 (Figure 42b) or 11174 (Figure 40b); postgenal bridge closed (Figure 2d). Gaster often with transverse rows of foveae and crenulations in *Ormyrus*, which comprises most of the diversity of the subfamily; metacoxae enlarged, flattened on the external surface and subtriangular in cross section (Figure 41e); metatibial spurs stout, curved; tarsal claw with or without a large basal projection; marginal vein at least 3.5× as long as postmarginal vein (Figure 42g).

Biology. Parasitoids of gall formers, especially hymenopterous gall formers.

Distribution. Worldwide.

Eubeckerella Narendran, 1999 (Figure 40).

Eubeckerella Narendran, 1999. **Type species**: *Eubeckerella malaica* Narendran, 1999.

REDEFINING ORMYRIDAE

Systematic
Entomology
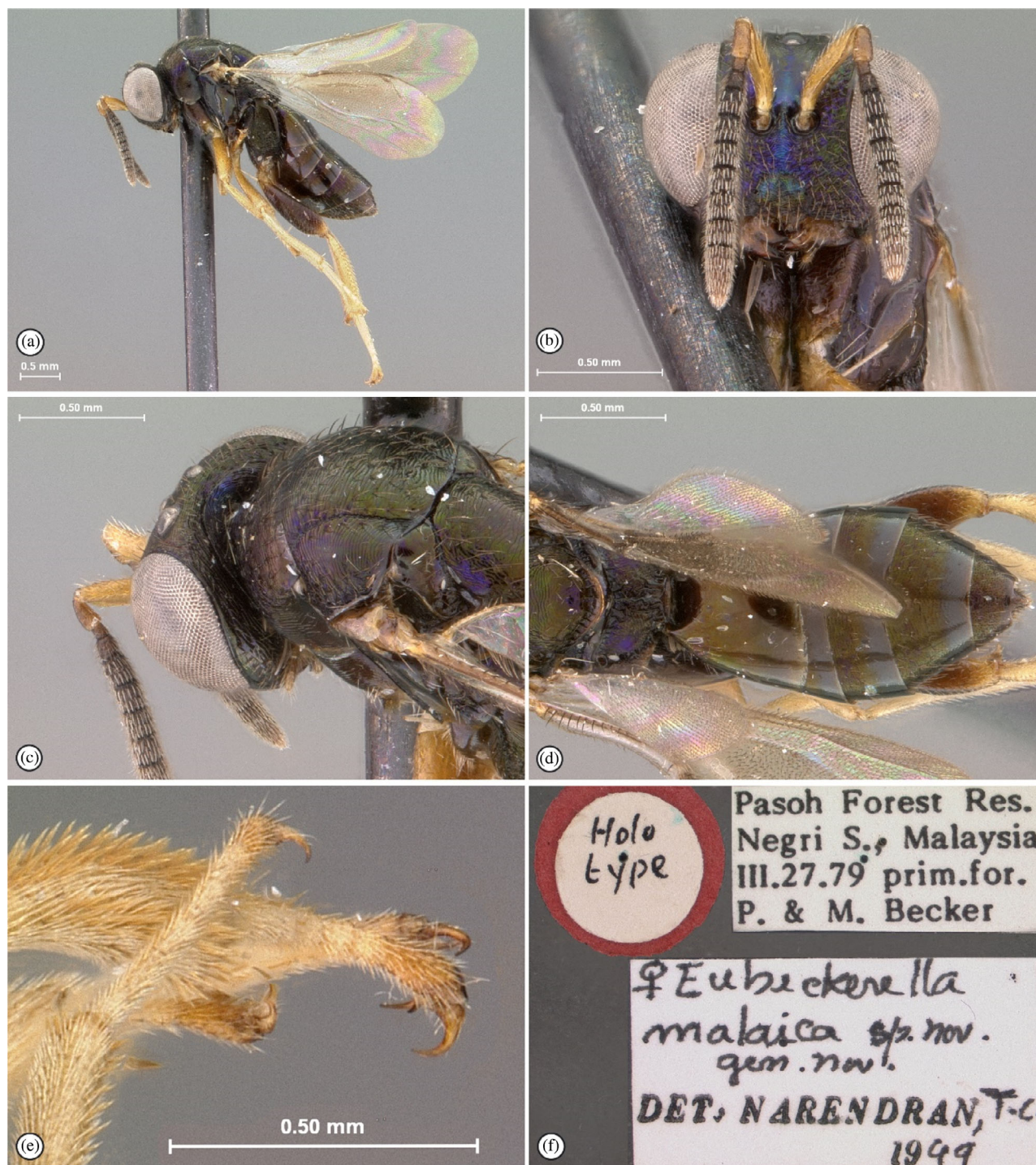
Royal
Entomological
Society

37

FIGURE 40 *Eubeckerella malaica* Narendran ♀ (AEI). (a) habitus, lateral view, (b) head, anterior view, (c) head, mesosoma, dorso–lateral view; (d) gaster, dorsal view; (e) tarsi and tarsal claws; (f) data labels.

Diagnosis. Eyes very large, hence malar space very short (Figure 40a); face mainly rugose–striate (Figure 40b); notauli deep in posterior part (Figure 40c); antennal formula 11174 (Figure 40b); fore wing with diffuse median infumation (Figure 40a); most gastral tergites weakly punctulate–reticulate, without any pits or crenulate borders (Figure 40d); cerci peg-like (Figure 40d); tarsal claws long and thin, sharply pointed with rudimentary basal swelling (Figure 40e).

Biology. Unknown.

Distribution. Malaysia.

Comments. Narendran (1999) states that *E. malaica* lacks an occipital carina, this being 'replaced by occipital groove' (p. 145) or 'occipital sulcus' (p. 147). This is a misinterpretation as the occipital carina is
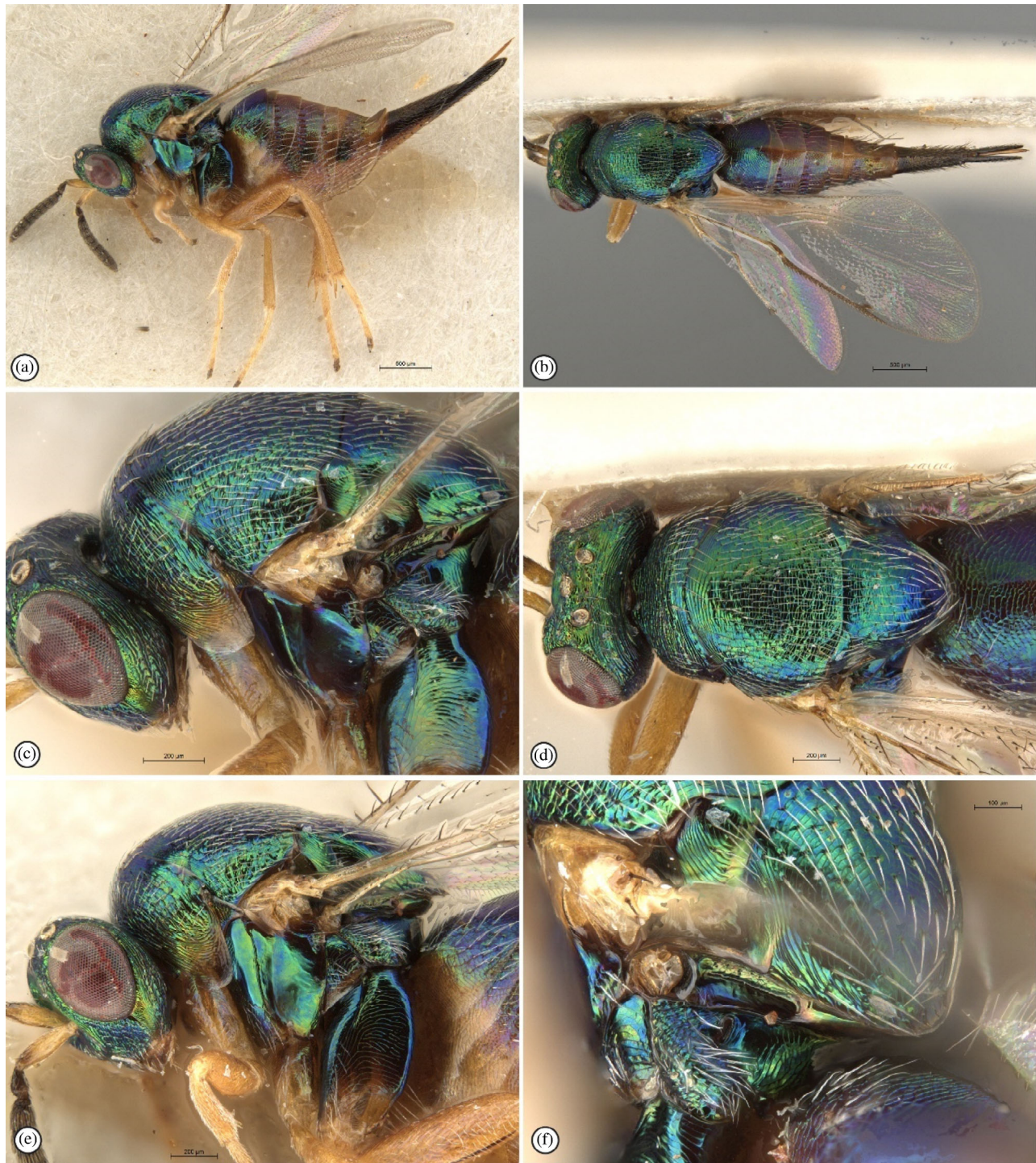
FIGURE 41 *Ormyrus flavipes* holotype ♀, B.M. TYPE HYM 5.2877 (NHMUK). (a) habitus, lateral view; (b) habitus, dorsal view; (c) head and mesosoma, dorso–lateral view; (d) head and mesosoma, dorsal view; (e) head and mesosoma, lateral view; (f) scutellum, propodeum, latero–dorsal view.

clearly present in the holotype specimen (Figure 40c). In other morphological respects, *Eubeckerella* fits within the delimitation of the Ormyrinae and hence, we reinstate the placement of this genus in the Ormyridae (left unplaced to family in Burks et al., 2022), and specifically within the nominate subfamily.

***Eubeckerella malaica* Narendran** (Figure 40).

Eubeckerella malaica Narendran, 1999. Holotype: ♀ in American Entomological Institute, Utah State University, Logan. Type Locality: Pasoh Forest Res., Negri S., Malaysia.

Diagnosis. The same as for the genus.

Biology. Unknown.

FIGURE 42 *Ormyrus flavipes* holotype ♀, B.M. TYPE HYM 5.2877 (NHMUK). (a) head, anterior view; (b) head and antennae, lateral view; (c) head and antenna, ventrolateral view; (d) metasomal tergites 1–6, lateral view; (e) metasoma, dorsal view; (f) metasoma, with terminal tergites and ovipositor in dorsal view; (g) wings (inset: data labels).

Distribution. Malaysia.

Ormyrus **Westwood** (Figures 41 and 42).

Ormyrus Westwood, 1832: 127. Type species: *Ormyrus punctiger* Westwood, 1832.
Periglyphus Boheman, 1834: 378. Synonymy by von Dalla Torre, 1898: 598.

Siphonura Nees ab Esenbeck, 1834: 81. Synonymy by von Dalla Torre, 1898: 598.
Cyrtosoma Perris, 1840: 96. Synonymy by Mayr, 1904: 565.
Cyrtosoma (*Monobaeus*) Förster, 1860. New status in Doganlar, 1991: 3.
Cyrtosoma (*Tribaeus*) Förster, 1860. New status in Doganlar, 1991: 3.
Tribaeus Förster, 1860: 93. Synonymy by Mayr, 1904: 565.

Monobaeus Förster, 1860: 95. Synonymy by Mayr, 1904: 560.

Torymus (*Chrysoideus*) De Stefani, 1898: 172. Synonymy by Risbec, 1954: 535.

Wania Risbec, 1951: 535. Synonymy by Peck, 1963: 591.

Avrasyamyrus Doganlar, 1991: 3, 7–8. Synonymy by Hanson, 1992: 1335.

Ormyrulus Bouček, 1986. Type species: *Ormyrulus gibbus* Bouček, 1986, **syn. nov**.

Diagnosis. Antenna with one to three anelli, five to seven funiculars and four clavomeres including the terminal button (Figure 42b); clypeus with apical margin bilobed (Figure 42a); occipital carina well developed (Figure 2d); postgenal lamina absent (Figure 2d); postgenal bridge closed (Figure 2d); metacoxa greatly enlarged, subtriangular in cross section (Figure 41e); metatibia with 2 stout curved spurs; tarsal claws with large basal lamellar projection; gaster heavily sclerotized, usually with transverse rows of large foveae (pits) basally on tergites (Figure 42d).

Comments on synonymy. Although Bouček (1986) mentioned in his description that *Ormyrulus* has no occipital carina, *O. gibbus* clearly has this carina. The carina was interpreted by Bouček (1986) as the 'sharp arcuate dorsal ridge separating the vertex from the steep shallowly excavated occiput' and although this carina is situated very high on the head it is clearly homologous with the occipital carina present in *Ormyrus* (Figure 39c). In all other morphological respects, *Ormyrulus* (Figure 39c,d) fits within the interpretation of *Ormyrus* and placement within the *Ormyrus* clade is corroborated by the molecular phylogenomic analyses, hence, we synonymise *Ormyrulus* with *Ormyrus*, resulting in the new combination *Ormyrus gibbus* (Bouček, 1986) **comb. nov.**

Biology. Parasitoids of various gall formers, especially Cynipidae (Hymenoptera) and Chalcidoidea (e.g., gall formers in syconia of Paleotropical figs), but also Cecidomyiidae and Tephritidae (Diptera) (Gomez et al., 2017; Hernández-Nieves, 2007; Noyes, 2019). *Ormyrus gibbus* (Bouček, 1986) is a parasitoid of *Procontarinia matteiana* (Cecidomyiidae), which forms galls on leaves of mango trees, *Mangifera indica* (Bouček, 1986).

Distribution. Worldwide.

Species richness.

Overall, 145 described species, including *Ormyrus gibbus* (Bouček, 1986), **comb. nov.**

Ouma Mitroiu, **gen. nov.** (Figures 45 and 46).

LSID urn:lsid:zoobank.org:act:CCF1BF41-8 BC2-4B2C-AB10-1B32 B4903D39.

Type species: *Ouma emazantsi* Mitroiu, **sp. nov.**

Diagnosis. Eyes normal, malar space long (Figures 45c and 46c); face mainly reticulate–imbricate (Figures 45c and 46c); notauli shallow to almost indistinct at least in posterior part (Figure 45b); antennal formula 11263 (Figure 45e); fore wing hyaline (Figure 45f); tarsal claw with cleft or uncleft basal projection; most metasomal tergites weakly punctulate–reticulate, without any pits or crenulate borders (Figure 45d); cerci peg-like.

Etymology. Named after the Afrikaans word *ouma* meaning grandmother, referring to the apparently plesiomorphic characters of this genus as compared to other Ormyrinae. Gender feminine.

Biology. Unknown.

Distribution: South Africa, Tanzania.

Description.

Head. Face uniformly reticulate–imbricate, except almost smooth clypeus (Figure 46c). Clypeus slightly produced, lower margin with a very weak emargination. Eyes normal (Figure 46c). Toruli higher than lower ocular line (Figure 46c). Scape reaching or almost reaching lower margin of median ocellus. Occipital carina fine. Antenna with formula 11,263 (Figure 46e).

Mesosoma. Pronotal collar slightly narrower than mesoscutum (Figure 46b). Mesoscutum predominantly striate-reticulate in anterior half and reticulate in posterior half; notauli hardly distinct, in posterior part as shallow depressions (Figure 45b), or more distinct but becoming shallower in posterior part (Figure 46b). Mesoscutellum reticulate; frenal area mostly not delimited and hardly or impossible to separate from rest of mesoscutellum. Metascutellum medially shiny, hidden under the expanded posterior margin of mesoscutellum. Propodeum irregularly sculptured (Figures 45d and 46d). Prepectus virtually smooth. Fore wing (Figure 46f) extensively bare in basal part; speculum large, gradually narrowing and reaching stigmal vein; veins slender; stigma elongate, with small uncus (Figure 46f). Hind leg with coxa plus trochanter about as long as femur (Figure 45a). Tarsal claw with cleft or uncleft basal projection.

Gaster. First tergite virtually smooth, the following tergites uniformly and shallowly punctulate–reticulate, except their smooth posterior margin (Figure 45d). Ovipositor sheaths not or slightly protruding.

Comments. The new genus appears to be closest to *Eubeckerella* due to its almost smooth gastral tergites, without any pits or crenulate borders. For the most important differences between the two genera, see the key to subfamilies and genera. In the holotype of *O. daleskeyae* the head has been reattached, with its posterior part covered in glue, so the occipital carina is not visible; however, because of many similarities between this species and *O. daleskeyae*, it is presumed that the shape of the occipital carina is similar in both species. One additional label of the *O. emazantsi* holotype states (in Bouček's handwriting): '? blisko fosilnimu rodu od Bachmaiera (barev fotografie)', which can be translated as '? close to fossil genus from Bachmaier (coloured photos)'. We are not aware of any work by this author that includes such a genus.

Key to *Ouma* species

Fig. 43

1. Notauli indistinct, in posterior part as very shallow depressions (Fig. 43A); median area of propodeum with weak irregular carinae, their interspaces rugose (Fig. 43B); upper part of scrobes and ocellar triangle rugose-reticulate, sculpture much denser than surrounding areas; second flagellomere quadrate (Fig. 43C); third flagellomere only slightly narrower than clava (Fig. 43C); tarsal claw projection cleft; flagellum dark brown (Fig. 43C); multiporous plate sensilla white, contrasting with flagellomeres (Fig. 43C); head and mesosoma dark blue-green (Fig. 43A) .... *O. daleskeyae* Mitroiu sp. nov.

Fig. 44

- Notauli distinct, although not deep (Fig. 44a); median area of propodeum with stronger irregular carinae, their interspaces almost smooth (Fig. 44b); upper part of scrobes and ocellar triangle reticulate, sculpture not much denser than surrounding areas; second flagellomere transverse (Fig. 44c); third flagellomere distinctly narrower than clava (Fig. 44c); tarsal claw projection uncleft; flagellum yellowish brown (Fig. 44c); multiporous plate sensilla pale brown, not contrasting with flagellomeres (Fig. 44c); head and mesosoma brownish, with olive green reflections (Fig. 44a) .... *O. emazantsi* Mitroiu, sp. nov.

Ouma daleskeyae Mitroiu, sp. nov. (Figure 45).
LSID urn:lsid:zoobank.org:act:5D2BD8A0-7C7F-4B36-B03B-0C12944D67E8.

Holotype. ♀. TANZANIA, Africa or. Katona, Arusha 1905. Deposited in NHMUK.

Diagnosis. Upper part of scrobes and ocellar triangle rugose–reticulate, sculpture much denser than surrounding areas (Figure 45e); notauli comparatively indistinct, in posterior part as very shallow depressions (Figure 45b); median area of propodeum with weak irregular carinae, their interspaces rugose (Figure 45d); first flagellomere transverse; second flagellomere quadrate; third flagellomere only slightly narrower than clava; flagellum dark brown; multiporous plate sensilla white, contrasting with flagellomeres (Figure 45e);

head and mesosoma dark blue–green (Figure 45c); fore wing hyaline (Figure 45f).

Etymology. The species is named for Natalie Dale-Skey, whose curatorial efforts lead to the discovery of many hidden treasures in the NHMUK collections. Noun in genitive case.

Biology. Unknown.

Distribution. Tanzania.

Description. Body length 2.5 mm.

Colour. Head and mesosoma mainly dark blue–green (Figure 45b); posterior margin of mesoscutellum light brown (Figure 45b). Gaster
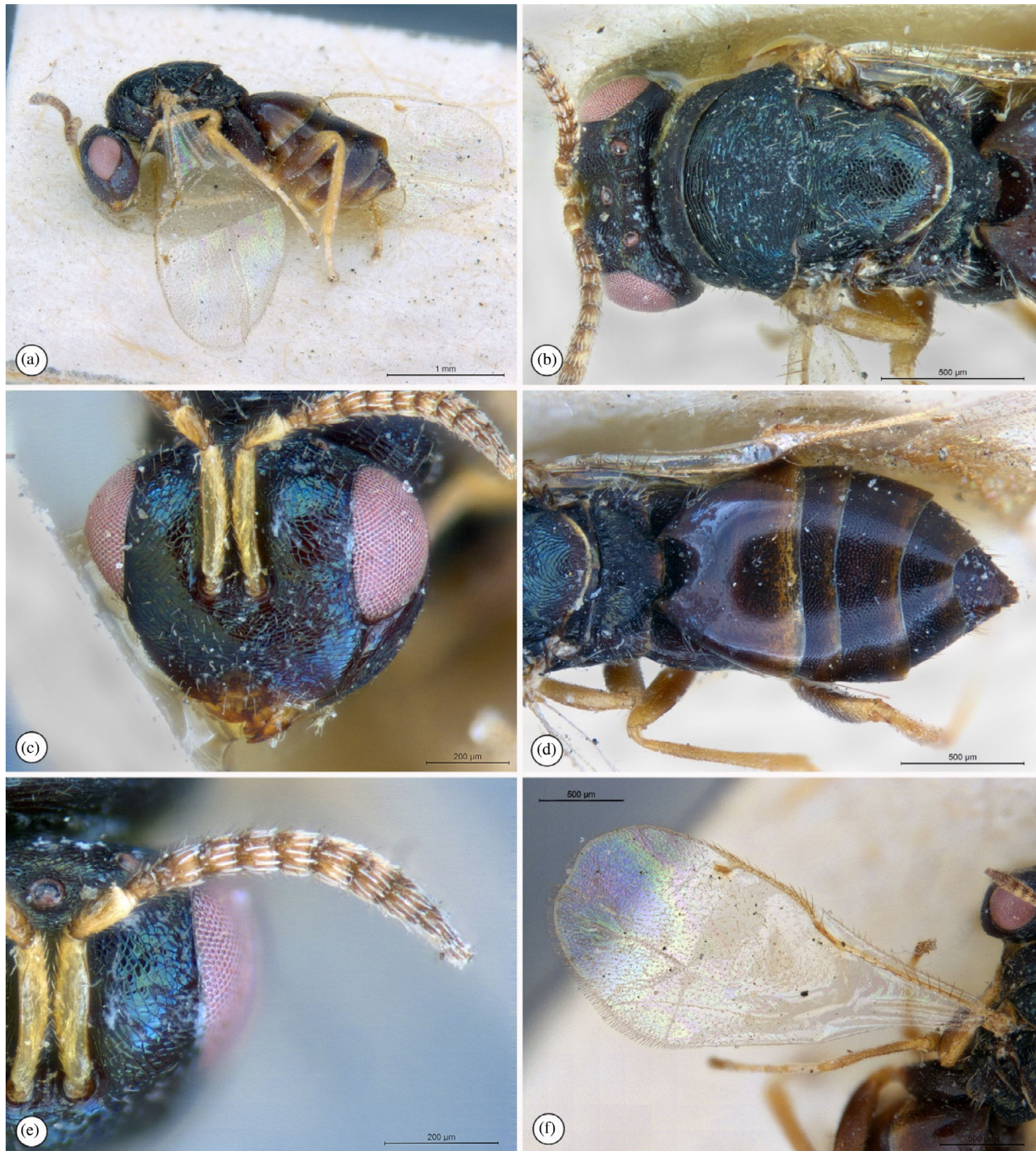
FIGURE 45 *Ouma daleskeyae* Mitroiu, **sp. nov**., holotype ♀ (NHMUK). (a) habitus, lateral view; (b) head, mesosoma, dorsal view; (c) head, frontal view; (d) propodeum, gaster, dorsal view; (e) antenna; (f) fore wing.

dark brown, with slight bluish reflections, ventrally paler (Figure 45d). Scape and pedicel yellowish, the latter dorsally brownish; flagellum dark brown, multiporous plate sensilla white, contrasting with flagellomeres (Figure 45e). Eyes pale reddish. Mandibles yellowish brown, teeth darker. Coxae concolorous with mesosoma; femora medially dark brown; tibiae and tarsi yellowish, apical tarsomere brown (Figure 45a). Wings hyaline; venation light brown (Figure 45f).

Head. Upper part of scrobes and ocellar triangle rugose–reticulate, sculpture much denser than surrounding areas (Figure 45e). Scape reaching above lower margin of median ocellus (Figure 45c). Relative measurements: head length: 35, width: 75, height: 60; eye height: 35, length: 26; malar space: 24; scape length: 29, width 6; pedicel length: 11, width: 5.5; pedicel plus flagellum length: 70; fl$_2$ length: 4, width: 4; fl$_8$ length: 7, width: 8; clava length: 19, width: 9.

FIGURE 46 *Ouma emazantsi* Mitroiu, **sp. nov**., holotype ♀ (NHMUK). (a) habitus, lateral view; (b) head, mesosoma, dorsal view; (c) head, antero–lateral view; (d) propodeum, gaster, dorsal view; (e) antenna; (f) fore wing.

Mesosoma. Pronotal collar striate–imbricate (Figure 45b). Mesoscutum predominantly striate in anterior half and reticulate in posterior half; notauli comparatively indistinct, as shallow depressions in posterior part (Figure 45b). Frenal area not delimited but with slightly shinier region occupying slightly less than half its length. Propodeal median area with several very fine irregular carinae, the interspaces between them rugose (Figure 45d). Mesopleuron and metapleuron mostly uniformly and finely reticulate. Tarsal claw projection cleft. Relative measurements: mesosoma length: 105, width: 76, height: 65; mesoscutum length: 38, width: 76; mesoscutellum length: 48, width: 43; propodeum length: 25; fore wing length: 250, width: 107; marginal vein: 43; stigmal vein: 10; postmarginal vein: 17.

Gaster. Ovipositor sheaths not protruding (Figure 45d). Relative measurements: gastral length: 130, width 80; first tergite length: 55, width: 80.

Ouma emazantsi Mitroiu, **sp. nov.** (Figure 46).
LSID   urn:lsid:zoobank.org:act:80363EEA-3F63-4B29-B6D8-6E661D3B7BC4.

Holotype. ♀. SOUTH AFRICA, Port St. John, Pondoland, Aug. 15–31. 1923. S. Africa. R. E. Turner, Brit. Mus. 1923–463. Deposited in NHMUK.

Diagnosis. Upper part of scrobes and ocellar triangle reticulate, the sculpture not much denser than surrounding areas; notauli distinct, shallow (Figure 46c); median area of propodeum with interspaces between irregular carinae smooth; first flagellomere transverse; second flagellomere transverse; third flagellomere distinctly narrower than clava; flagellum yellowish brown; multiporous plate sensilla pale brown, not contrasting with flagellomeres (Figure 46e); head and mesosoma brownish, with olive green reflections (Figure 46b); fore wing hyaline (Figure 46f).

Etymology. In Xhosa language, *emazantsi* means 'southern', with reference to the species' known distribution. Noun in apposition.

Biology. Unknown.

Distribution. South Africa.

Description. Body length 1.75 mm.

Colour. Body brownish, with distinct olive green reflections on face, vertex and dorsal side of mesosoma (Figure 46a). Scape and pedicel pale yellow except pedicel dorsally brownish; flagellum yellowish brown, multiporous plate sensilla pale brown, not contrasting with flagellomeres (Figure 46e). Eyes dark red. Mandibles yellowish brown, the teeth darker. Coxae concolorous with mesosoma, the procoxae slightly lighter; femora light brown; tibiae and tarsi yellowish except, apical tarsomeres brown (Figure 46a). Wings hyaline; venation light brown (Figure 46f).

Head. Upper part of scrobes and ocellar triangle reticulate, the sculpture not denser than surrounding areas. Scape almost reaching lower margin of median ocellus. Relative measurements: head length: 35, width: 70, height: 55; eye height: 34, length: 26; malar space: 25; scape length: 27, width 5.5; pedicel length: 10, width: 5; pedicel plus flagellum length: 63; fl_2 length: 3.5, width: 4.5; fl_8 length: 6, width: 8; clava length: 18, width: 10.

Mesosoma. Pronotal collar imbricate–reticulate (Figure 46b). Mesoscutum predominantly striate-reticulate in anterior half and reticulate in posterior half; notauli distinct, becoming shallower in posterior part (Figure 46b). Frenal area not delimited.

Propodeal median area with several conspicuous irregular carinae, the interspaces between them almost smooth. Mesopleuron very delicately reticulate, lower mesepimeron almost smooth. Metapleuron uniformly reticulate. Tarsal claw projection uncleft. Relative measurements: mesosoma length: 98, width: 61, height: 58; mesoscutum length: 35, width: 61; mesoscutellum length: 42, width: 35; propodeum length: 20; fore wing length: 210, width: 90; marginal vein: 39; stigmal vein: 9; postmarginal vein: 15.

Gaster. Ovipositor sheaths slightly protruding. Relative measurements: gastral length: 100, width: 61; first tergite length: 50, width: 61.

DISCUSSION

Molecular analyses of relationships and re-interpretation of morphological character states within the Chalcidoidea have demonstrated the necessity for a radical reconfiguration of the historical classification of the superfamily (Burks et al., 2022; Cruaud et al., 2024). The circumscription of Ormyridae as proposed by Burks et al. (2022) and modified here is strongly supported by phylogenomic molecular analyses of UCEs and their flanking regions (IQ-TREE SH-aLRT ≥80/ UFBoot ≥95; ASTRAL local PP ≥0.9). In turn, the relationships indicated by the molecular analyses are corroborated by comparative morphological assessment of shared character states, particularly based on such previously overlooked characters as the structure of the posterior of the head, the lateral panel of the prepectus and tarsal claw configuration. The relative structural arrangement of the lateral panel of the prepectus is a synapomorphy grouping all six ormyrid genera and is a unique configuration within the Chalcidoidea.

The morphological analysis justified the previous transfer of *Asparagobius* and *Hemadas* to Ormyridae as well as placement of the newly described genus *Halleriaphagus* in the family. There is, however, sufficient divergence within the components of the newly defined Ormyridae to justify the recognition of subfamilies to compartmentalize the three clades nomenclaturally. Hemadinae were recovered as a sister group to the Asparagobiinae and Ormyrinae. The basal clades comprising the Hemadinae and Asparagobiinae are represented by primary gall formers, with the shift to a parasitoid lifestyle thus probably being a derived trait present only in the Ormyrinae. This preliminary hypothesis would need to be thoroughly assessed through the inclusion of a substantial portion of the 145 known *Ormyrus* species in a phylogenetic analysis. Of interest is the correlated association of *Asparagobius braunsi* and an undescribed *Ormyrus* species developing simultaneously in the same gall formed on *Asparagus* (van Noort, unpublished data), meaning that if *Asparagobius* is the primary gall former then *Ormyrus* likely is a parasitoid of *Asparagobius* in this case. Given the close evolutionary relationship of these genera, this biological relationship could potentially be a case of agastoparasitism as demonstrated for cynipid inquilines (Ronquist, 1994).

The specialist fig (*Ficus*, Moraceae) associated Epichrysomallidae were recovered as the sister group to the newly defined Ormyridae.

Most species of Epichrysomallidae gall the florets within the fig cavity early on in fig development. They oviposit through the fig wall prior to the pollinators arriving at receptive figs and are subsequently parasitized by species of *Sycophila* (Eurytomidae) (Compton & van Noort, 1992; Kerdelhué et al., 2000; Segar et al., 2013). However, a few species of Epichrysomallidae form galls in the fig walls or in the terminal leaf buds or, more rarely, on the roots or twigs (Beardsley & Rasplus, 2001; Ferrière, 1929). Several *Ormyrus* species are associated with figs and our phylogeny suggests that these are an independent subsequent re-colonization of the fig niche. Like the epichrysomallids they also develop within galls in the fig or in aerial root galls or in leaf terminal galls (Bouček et al., 1981; Noyes, 2019) and are surmised to be attacking the epichrysomallids developing in these niches.

More inclusive coverage of representatives of the species-rich genus *Ormyrus* in phylogenomic analyses would allow for mapping of the known biological lifestyle strategies onto the resulting cladogram, providing elucidation of the seemingly complex evolutionary history of biology within the family.

ICZN COMPLIANCE

New nomenclatural acts contained herein conform to the articles and recommendations of the International Code of Zoological Nomenclature.

AUTHOR CONTRIBUTIONS

Simon van Noort: Conceptualization; investigation; funding acquisition; writing – original draft; methodology; validation; visualization; software; data curation; resources; writing – review and editing. **Mircea-Dan Mitroiu:** Conceptualization; investigation; writing – review and editing; methodology; validation; visualization; data curation. **Roger Burks:** Conceptualization; investigation; writing – review and editing; visualization; validation; methodology; data curation. **Gary Gibson:** Conceptualization; investigation; writing – review and editing; visualization; validation; methodology. **Paul Hanson:** Conceptualization; investigation; writing – review and editing; visualization; validation; methodology. **John Heraty:** Conceptualization; investigation; writing – review and editing; visualization; validation; methodology. **Petr Janšta:** Conceptualization; investigation; methodology; validation; visualization; writing – review and editing. **Astrid Cruaud:** Conceptualization; investigation; funding acquisition; methodology; validation; visualization; writing – review and editing; software; formal analysis; data curation; resources. **Jean-Yves Rasplus:** Conceptualization; investigation; funding acquisition; methodology; validation; visualization; writing – review and editing; software; formal analysis; data curation; resources.

ACKNOWLEDGEMENTS

FUNDING INFORMATION

CONFLICT OF INTEREST STATEMENT

All authors declare no conflict of interest.

DATA AVAILABILITY STATEMENT

Raw paired reads for UCEs were uploaded as NCBI Sequence Read Archives (BioProject PRJNA1068600). Data set and trees are available on Zenodo (https://doi.org/10.5281/zenodo.10566819).

ETHICS STATEMENT

The required permits were obtained from the relevant authorities for collection and export of specimens. Cape Nature (Western Cape Province), the Eastern Cape Department of Environmental Affairs, the Northern Cape Department of Nature and Environmental Conservation (South Africa) and the Queensland parks and wildlife services (Australia).

ORCID

Simon van Noort https://orcid.org/0000-0001-6930-9741
Mircea-Dan Mitroiu https://orcid.org/0000-0003-1368-7721
Roger Burks https://orcid.org/0000-0003-3032-7939
Gary Gibson https://orcid.org/0000-0002-8161-7445
Paul Hanson https://orcid.org/0000-0002-7667-7718
John Heraty https://orcid.org/0000-0002-9246-5651
Petr Janšta https://orcid.org/0000-0001-6409-3603
Astrid Cruaud https://orcid.org/0000-0001-8932-4199
Jean-Yves Rasplus https://orcid.org/0000-0001-8614-6665

REFERENCES

Ashmead, W.H. (1887) Studies on the North American Chalcididae, with descriptions of new species, chiefly from Florida. *Transactions of the American Entomological Society*, 14, 183–203.

Ashmead, W.H. (1904) Classification of the chalcid flies, or the superfamily Chalcidoidea, with descriptions of new species in the Carnegie museum, collected in South America by Herbert H Smith. *Memoirs of the Carnegie Museum*, 1, 225–551.

Askew, R.R. & Blasco-Zumeta, J. (1998) Insects associated with galls of a new species of Eurytomidae (Hymenoptera: Chalcidoidea) on *Ephedra nebrodensis* in Spain. *Journal of Natural History*, 32, 805–821.

Askew, R.R., Plantard, O., Gómez, J.F.H., Nieves, M. & Nieves-Aldrey, J.L. (2006) Catalogue of parasitoids and inquilines in galls of Aylacini, Diplolepidini and Pediaspidini (Hym., Cynipidae) in the West Palaearctic. *Zootaxa*, 1301, 1–60.

Beardsley, J.W. & Rasplus, J.Y. (2001) A new species of *Josephiella* (Hymenoptera: Agaonidae) forming leaf galls on *Ficus microcarpa* L. (Moraceae). *Journal of Natural History*, 35, 33–40.

Blaimer, B.B., Santos, B.F., Cruaud, A., Gates, M.W., Kula, R.R., Mikó, I. et al. (2023) Key innovations and the diversification of Hymenoptera. *Nature Communications*, 14, 1212.

Boheman, C.H. (1834) Skandinaviska Pteromaliner. *Kongliga Vetenskaps-Akademiens Handlingar*, 1833, 378.

Bolger, A.M., Lohse, M. & Usadel, B. (2014) Trimmomatic: a flexible trimmer for Illumina sequence data. *Bioinformatics*, 30, 2114–2120.

Bouček, Z. (1986) Taxonomic study of chalcidoid wasps (Hymenoptera) associated with gall midges (Diptera: Cecidomyiidae) on mango trees. *Bulletin of Entomological Research*, 76, 393–407.

Bouček, Z. (1988) *Australasian Chalcidoidea (Hymenoptera). A biosystematic revision of genera of fourteen families, with a reclassification of species*. Wallingford, United Kingdom: CAB International, p. 832.

Bouček, Z., Watsham, A. & Wiebes, J.T. (1981) The fig wasp fauna of the receptacles of *Ficus thonningii* (Hymenoptera, Chalcidoidea). *Tijdschrift voor Entomologie*, 124, 149–233.

Bunnefeld, L., Hearn, J., Stone, G.N. & Lohse, K. (2018) Whole-genome data reveal the complex history of a diverse ecological community. *Proceedings of the National Academy of Sciences of the United States of America*, 115, E6507–E6515.

Burks, R.A., Mitroiu, M.-D., Fusu, L., Heraty, J.M., Janšta, P., Heydon, S. et al. (2022) From hell's heart I stab at thee! A determined approach towards a monophyletic Pteromalidae and reclassification of Chalcidoidea (Hymenoptera). *Journal of Hymenoptera Research*, 94, 13–88.

Compton, S.G. & van Noort, S. (1992) Southern African fig wasps (Hymenoptera: Chalcidoidea): resource utilization and host relationships. *Proceedings of the Koninklijke Nederlandse Akademie van Wetenschappen. Series C. Biological and Medical Sciences*, 95, 423–435.

Cooper, W.R. & Rieske, L.K. (2011) A native and an introduced parasitoid utilize an exotic gall-maker host. *BioControl*, 56, 725–734.

Crawford, J.C. (1909) Notes on some Chalcidoidea. *Canadian Entomologist*, 41(3), 98.

Cruaud, A., Nidelet, S., Arnal, P., Weber, A., Fusu, L., Gumovsky, A. et al. (2019) Optimized DNA extraction and library preparation for minute arthropods: application to target enrichment in chalcid wasps used for biocontrol. *Molecular Ecology Resources*, 19, 702–710.

Cruaud, A., Rasplus, J.-Y., Zhang, J., Burks, R., Delvare, G., Fusu, L. et al. (2024) The Chalcidoidea bush of life—evolutionary history of a massive radiation of minute wasps. *Cladistics*, 40, 34–63. Available from: https://doi.org/10.1111/cla.12561

De Stefani, T. (1898) Note intorno ad alcuni zoocecidii del *Quercus robur* e del *Q. suber* raccolti nel territorio di Castelvetrano (Sicilia). *Naturalista Siciliano*, 2, 156–174.

Doganlar, M. (1991) Systematic positions of some taxa in Ormyridae and descriptions of a new species in *Ormyrus* from Turkey and a new genus in the family (Hymenoptera, Chalcidoidea). *Türkiye Entomoloji Dergisi*, 15(1), 1–13.

Fabricius, J.C. (1804) *Systema Piezatorum*, Vol. 2. A.C. Reichard, Brunsvigae, p. 163.

Faircloth, B.C., Branstetter, M.G., White, N.D. & Brady, S.G. (2015) Target enrichment of ultraconserved elements from arthropods provides a genomic perspective on relationships among Hymenoptera. *Molecular Ecology Resources*, 15, 489–501.

Ferrière, C. (1929) Chalcidiens gallicoles de Java. *Annales de la Société Entomologique de France*, 48, 143–161.

Förster, A. (1856) II. Chalcidiae und Proctotrupii. In: *Hymenopterologische Studien*. Aachen, Germany: Ernst ter Meer, p. 152.

Förster, A. (1860) Eine centurie neuer Hymenopteren. *Verhandlungen des Naturhistorischen Vereins der Preussischen Rheinlande und Westfalens, Bonn*, 17, 93.

Gahan, A.B. & Ferrière, C. (1947) Notes on some gall-inhabiting Chalcidoidea (Hymenoptera). *Annals of the Entomological Society of America*, 40(2), 271–302 Pl. I & II.

Gascuel, O. (1997) BIONJ: an improved version of the NJ algorithm based on a simple model of sequence data. *Molecular Biology and Evolution*, 14(7), 685–695. Available from: https://doi.org/10.1093/oxfordjournals.molbev.a025808

Gibbs Russell, G.E., Welman, W.G.M., Retief, E., Immelman, K.L., Germishuizen, G., Pienaar, B.J. et al. (1987) List of species of southern African plants. *Memoirs of the Botanical Survey of South Africa*, 2(1–2), 1–152(pt. 1)–1–270(pt. 2).

Gibson, G.A.P. (1997) Morphology and terminology. In: Gibson, G.A.P., Huber, J.T. & Woolley, J.B. (Eds.) *Annotated keys to the genera of Nearctic Chalcidoidea (Hymenoptera): 16–44*. Ottawa: NRC Research Press.

Gil-Tapetado, D., Cabrero-Sañudo, F.J., Gómez, J.F., Askew, R.R. & Nieves-Aldrey, J.L. (2021) Differences in native and introduced chalcid parasitoid communities recruited by the invasive chestnut pest *Dryocosmus kuriphilus* in two Iberian territories. *Bulletin of Entomological Research*, 111, 307–322.

Girault, A.A. (1915) Australian Hymenoptera Chalcidoidea, XII. The family Callimomidae with descriptions of new genera and species. *Memoirs of the Queensland Museum*, 4, 275–309.

Girault, A.A. (1917) *Descriptions hymenopterorum chalcidoidicarum variorum cum observationibus. V.* Glenndale, Maryland: Private Publication, p. 2.

Gomez, J.F., Nieves, M.H., Gayubo, S.F. & Nieves-Aldrey, J.L. (2017) Terminal-instar larval systematics and biology of west European species of Ormyridae associated with insect galls (Hymenoptera, Chalcidoidea). *Zookeys*, 644, 51–88. Available from: https://doi.org/10.3897/zookeys.644.10035

Guindon, S., Dufayard, J.F., Lefort, V., Anisimova, M., Hordijk, W. & Gascuel, O. (2010) New algorithms and methods to estimate maximum-likelihood phylogenies: assessing the performance of PhyML 3.0. *Systematic Biology*, 59, 307–321.

Hanson, P. (1992) The Nearctic species of *Ormyrus* Westwood (Hymenoptera: Chalcidoidea: Ormyridae). *Journal of Natural History*, 26, 1333–1365. Available from: https://doi.org/10.1080/00222939200770761

Harris, R.A. (1979) A glossary of surface sculpturing. *Occasional Papers in Entomology*, 28, 1–31.

Harris, R.S. (2007) *Improved pairwise alignment of genomic DNA [PhD Thesis]*. State College: The Pennsylvania State University.

Hernández-Nieves, M. (2007) *Taxonomía, biología y filogenia de las especies ibéricas de Ormyridae [Tesis Doctoral]*. Salamanca: Universidad de Salamanca, p. 348.

Huang, X. & Madan, A. (1999) CAP3: A DNA sequence assembly program. *Genome Research*, 9, 868–877.

Isaacs, R., Fanning, P., van Timmeren, S., Perkins, J. & Garcia-Salazar, C. (2020) Biology and management of stem gall wasp in highbush blueberries. Michigan State University Extension Bulletin E3443.

Ito, M. & Hijii, N. (2000) Life-history traits in the parasitoid complex associated with cynipid galls on three species of Fagaceae. *Entomological Science*, 3, 471–479.

Kalyaanamoorthy, S., Minh, B.Q., Wong, T.K.F., von Haeseler, A. & Jermiin, L.S. (2017) ModelFinder: fast model selection for accurate phylogenetic estimates. *Nature Methods*, 14, 587–589.

Katoh, K. & Standley, D.M. (2013) MAFFT multiple sequence alignment software version 7: improvements in performance and usability. *Molecular Biology and Evolution*, 30, 772–780.

Kerdelhué, C., Rossi, J.-P. & Rasplus, J.-Y. (2000) Comparative community ecology studies on Old World figs and fig wasps. *Ecology*, 81, 2832–2849.

Lanfear, R., Frandsen, P.B., Wright, A.M., Senfeld, T. & Calcott, B. (2017) PartitionFinder 2: new methods for selecting partitioned models of evolution for molecular and morphological phylogenetic analyses. *Molecular Biology and Evolution*, 34, 772–773.

LaSalle, J. (1987) New World Tanaostigmatidae (Hymenoptera, Chalcidoidea). *Contributions of the American Entomological Institute*, 23(1), 1–181.

LaSalle, J. (2005) Biology of gall inducers and evolution of gall induction in Chalcidoidea (Hymenoptera: Eulophidae, Eurytomidae, Pteromalidae, Tanaostigmatidae, Torymidae). In: Raman, A., Schaefer, C.W. & Withers, T.M. (Eds.) *Biology, ecology, and evolution of gall-inducing arthropods*. Enfield, NH: Science Publishers, Inc, pp. 507–537.

Lateef, S.S., Reed, W. & LaSalle, J. (1985) *Tanaostigmodes cajaninae* LaSalle, sp. n. (Hymenoptera: Tanaostigmatidae), a potential pest of pigeon pea in India. *Bulletin of Entomological Research*, 75, 305–313.

MacKay, I.F. (1989) Oviposition behaviour of the gall inducer *Hemadas nubilipennis* (Hymenoptera: Pteromalidae). *Proceedings of the Entomological Society of Ontario*, 119, 93.

Magoc, T. & Salzberg, S.L. (2011) FLASH: fast length adjustment of short reads to improve genome assemblies. *Bioinformatics*, 27, 2957–2963.

Mai, U. & Mirarab, S. (2018) TreeShrink: fast and accurate detection of outlier long branches in collections of phylogenetic trees. *BMC Genomics*, 19, 272.

Mayr, G. (1904) Hymenopterologische miszellen. III. *Verhandlungen der Zoologisch-Botanischen Gesellschaft in Wien*, 54, 559–598.

Mayr, G. (1905) Hymenopterologische miszellen. IV. *Verhandlungen der Zoologisch-Botanischen Gesellschaft in Wien*, 55, 529–575.

McAlister, L.C. & Anderson, W.H. (1932) The blueberry stem-gall in Maine. *Journal of Economic Entomology*, 25, 1164–1169.

Minh, B.Q., Schmidt, H.A., Chernomor, O., Schrempf, D., Woodhams, M.D., von Haeseler, A. et al. (2020) IQ-TREE 2: new models and efficient methods for phylogenetic inference in the genomic era. *Molecular Biology and Evolution*, 37, 1530–1534.

Mirarab, S., Nguyen, N. & Warnow, T. (2014) PASTA: ultra-large multiple sequence alignment. *Research in Computational Molecular Biology*, 22, 177–191.

Mucina, L. & Ruthaford, M.C. (2006) *The vegetation of South Africa, Lesotho and Swaziland*. Pretoria: Strelitzia 19. South African National Biodiversity Institute.

Narendran, T.C. (1999) *Indo-Australian Ormyridae (Hymenoptera: Chalcidoidea)*. Kerala: Department of Zoology, University of Calicut, p. iii +227 pp. privately published, Narendran, T.C.

Nees ab Esenbeck, C.G. (1834) *Hymenopterorum ichneumonibus affinium, Monographiae, genera Europaea et species illustrantes*, Vol. 2. Stuttgart und Tübingen: sumptibus J.G. Cottæ, pp. 1–81.

Noyes, J.S. (2019) Universal Chalcidoidea Database. Available at: https://www.nhm.ac.uk/our-science/data/chalcidoids/database/ [Accessed 29th April 2022].

Peck, O. (1963) A catalogue of the Nearctic Chalcidoidea (Insecta; Hymenoptera). *Canadian Entomologist (Supplement)*, 30, 1–1092.

Penev, L., Sharkey, M., Erwin, T., van Noort, S., Buffington, M., Seltmann, K. et al. (2009) Data publication and dissemination of interactive keys under the open access model. *ZooKeys*, 21, 1–17. Available from: https://doi.org/10.3897/zookeys.21.274

Perris, E. (1840) Observations sur les insectes que habitent les galles de l'*Ulex nanus* et du *Papaver dubium*. *Annales de la Société Entomologique de France*, 9, 96.

Rasplus, J.-Y., Blaimer, B.B., Brady, S.G., Burks, R.A., Delvare, G., Fisher, N. et al. (2020) A first phylogenomic hypothesis for Eulophidae (Hymenoptera, Chalcidoidea). *Journal of Natural History*, 54, 597–609.

Rasplus, J.-Y., Harry, M., Perrin, H., Chassagnard, M.T. & Lachaise, D. (2003) Les *Ficus* (Moraceae) et l'entomofaune des figues (Hym. Agaonidae, Pteromalidae, Torymidae, Eurytomidae; Dipt. Drosophilidae; Col. Curculionidae) du mont Nimba en Guinée. In: Lamotte, M. & Roy, R. (Eds.) *Le peuplement animal du mont nimba, Guinée, Cote d'Ivoire, Liberia*, Vol. 190. Paris: Mémoires du Muséum national d'Histoire naturelle, pp. 146–147.

Rasplus, J.Y., LaSalle, J., Delvare, G., McKey, D. & Webber, B.L. (2011) A new Afrotropical genus and species of Tetrastichinae (Hymenoptera: Eulophidae) inducing galls on *Bikinia* (Fabaceae: Caesalpinioideae) and a new species of *Ormyrus* (Hymenoptera: Ormyridae) associated with the gall. *Zootaxa*, 2907, 51–59.

Rasplus, J.-Y., Nieves-Aldrey, J.L. & Cruaud, A. (2022) *Cecinothofagus* Nieves-Aldrey & Liljeblad (Hymenoptera, Cynipidae) is likely an endoparasitoid of the gall-maker genus *Aditrochus* Rübsaamen (Hymenoptera, Pteromalidae). *Journal of Hymenoptera Research*, 93, 33–42.

Risbec, J. (1951) 1. Les Chalcidoides de l'Afrique occidentale française. *Mémoires de l'Institute Français d'Afrique Noire, Ifan-Dakar*, 13, 7–409.

Risbec, J. (1954) Chalcidoïdes et proctotrupoïdes de l'Afrique occidentale française (3e supplément). *Bulletin de l'Institut Français d'Afrique Noire (A)*, 16, 524–552.

Ronquist, F. (1994) Evolution of parasitism among closely related species: phylogenetic relationships and the origin of inquilinism in gall wasps (Hymenoptera, Cynipidae). *Evolution*, 48, 241–266. Available from: https://doi.org/10.1111/j.1558-5646.1994.tb01310.x

Segar, S.T., Pereira, R.A., Compton, S.G. & Cook, J.M. (2013) Convergent structure of multitrophic communities over three continents. *Ecology Letters*, 16, 1436–1445.

Shanower, T.G., Lal, S.S. & Bhagwat, V.R. (1998) Biology and management of *Melanagromyza obtusa* (Malloch) (Diptera: Agromyzidae). *Crop Protection*, 17, 249–263.

Shimbori, E.M., Onody, H.C., Fernandes, D.R.R., Silvestre, R., Tavares, M.T. & Penteado-Dias, A.M. (2017) Hymenoptera "Parasitica" in the state of Mato Grosso do Sul, Brazil. *Iheringia, Serie Zoologia*, 107, e2017121.

Shorthouse, J.D., Mackay, I.F. & Zmijowkyj, T.J. (1990) Role of parasitoids associated with galls induced by *Hemadas nubilipennis* (Hymenoptera: Pteromalidae) on lowbush blueberry. *Environmental Entomology*, 19, 911–915.

Shorthouse, J.D., West, A., Landry, R.W. & Thibodeau, P.D. (1986) Structural damage by female *Hemadas nubilipennis* (Hymenoptera, Pteromalidae) as a factor in gall induction on lowbush blueberry. *The Canadian Entomologist*, 118, 249–254.

Singh, S. (2008) First record of the genus *Cynipencyrtus* Ishii (Hymenoptera: Tanaostimatidae) from India with description of a new species from Garhwal Himalayas. *Annals of Entomology*, 26, 59–63.

Tachikawa, T. (1973) Discovery of the hosts of *Cynipencyrtus bicolor* Ishii and *Microterys tarumiensis* Tachikawa (Hymenoptera: Chalcidoidea—Encyrtidae). *Transactions of the Shikoku Entomological Society*, 11(4), 133–134.

Tachikawa, T. (1978) A note on the genus *Cynipencyrtus* Ishii (Hymenoptera: Chalcidoidea—Encyrtidae). *Transactions of Shikoku Entomological Society*, 14(1/2), 69–71.

Tagliacollo, V.A., Lanfear, R. & Townsend, J. (2018) Estimating improved partitioning schemes for ultraconserved elements. *Molecular Biology and Evolution*, 35, 1798–1811.

Thomson, C.G. (1876) *Hymenoptera Scandinaviae IV*. Lund, Sweden: H.O. Boktryckeri, p. 192.

UCDW. (2023) Universal chalcidoidea database web (UCDW) curated in TaxonWorks. Available at: www.ucd.chalcid.org [Accessed 29th September 2023].

van Noort, S. (2023) Waspweb. https://www.waspweb.org [Accessed 16th September 2023].

van Noort, S. & Copeland, R.S. (2020) First record of the genus *Tanaostigma* (Hymenoptera, Chalcidoidea, Tanaostigmatidae) from the Afrotropical region with description of three new species. *Journal of Natural History*, 54(9–12), 703–722.

von Dalla Torre, K.W. (1898) *Catalogus Hymenopterorum hucusque descriptorum systematicus et synonymicus*. Leipzig: V. Chalcididae et Proctotrupidae, p. 598.

West, A. & Shorthouse, J.D. (1989) Initiation and development of the stem gall induced by *Hemadas nubilipennis* (Hymenoptera: Pteromalidae) on lowbush blueberry, *Vaccinium angustifolium* (Ericaceae). *Canadian Journal of Botany*, 67, 2187–2198.

Westwood, J.O. (1832) Descriptions of several new British forms amongst the parasitic hymenopterous insects. *Philosophical Magazine*, 1(3), 127–129.

Yao, Y.Y. & Yang, Z. (2004) A new species of Ormyridae (Hymenoptera: Chalcidoidea) parasitizing a gall-making weevil on twigs of the bunge hackberry tree in China. *Entomologica Fennica*, 15, 142–148.

Yoder, M.J., Mikó, I., Seltmann, K.C., Bertone, M.A. & Deans, A.R. (2010) A gross anatomy ontology for Hymenoptera. *PLoS ONE*, 5(12), e15991. Available from: https://doi.org/10.1371/journal.pone.0015991

Zerova, M.D. & Seryogina, L.Y. (2015) Ormyridae (Hymenoptera, Chalcidoidea, Ormyridae) of Palaearctic. *Vestnik Zoologii*, 32, 1–116.

Zhang, C., Rabiee, M., Sayyari, E. & Mirarab, S. (2018) ASTRAL-III: polynomial time species tree reconstruction from partially resolved gene trees. *BMC Bioinformatics*, 19, 153.

Zhu, Q. (2014) AfterPhylo. A perl script for manipulating trees after phylogenetic reconstruction. Available at: https://github.com/qiyunzhu/AfterPhylo/

SUPPORTING INFORMATION

Additional supporting information can be found online in the Supporting Information section at the end of this article.

Figure S1. Phylogenetic trees. (A) IQ-TREE tree obtained from the UCE data set without partitioning. SH-aLRT/UFBoot are shown at nodes. (B) IQ-TREE tree obtained from the UCE data set with partitioning using the SWSC method and the best partitioning scheme inferred by PartitionFinder. SH-aLRT/UFBoot are shown at nodes. (C) ASTRAL tree obtained from the 671 gene trees. Local posterior probabilities are shown at nodes.

Table S1. UCE sample details. Spreadsheet of UCEs obtained from previous publications (Blaimer et al., 2023; Cruaud et al., 2024; Rasplus et al., 2020; Rasplus et al., 2022), extracted from genomes (Bunnefeld et al., 2018) or captured de novo for the purpose of this study.

Table S2. Matrix of character states scored across the six genera considered to belong to the revised concept of the family Ormyridae.

Appendix S1. Lucid Interchange Format version 3 (LIF3) of the WaspWeb online Lucid matrix identification key to Ormyridae genera (Chalcidoidea, Hymenoptera).

The LIF3 file is an XML-based file that stores all the Lucid3 key data, allowing exchange of the key with other key developers. Copyright notice: This dataset is made available under the Open Database Licence (http://opendatacommons.org/licenses/odbl/1.0/). The Open Database Licence (ODbL) is a licence agreement intended to allow users to freely share, modify and use this Dataset while maintaining this same freedom for others, provided that the original source and author(s) are credited.